ORNL/TM-2021/2366

Light Water Reactor LEU+ Lattice Optimization

Jin Whan Bae
Ugur Mertyurek
Mehdi Asgari

September 1, 2022

OAK RIDGE National Laboratory

ORNL IS MANAGED BY UT-BATTELLE LLC FOR THE US DEPARTMENT OF ENERGY

ORNL/TM-2021/2366

Nuclear Energy and Fuel Cycle Division

LIGHT WATER REACTOR LEU+ LATTICE OPTIMIZATION

Jin Whan Bae
Ugur Mertyurek
Mehdi Asgari

September 1, 2022

Prepared by
OAK RIDGE NATIONAL LABORATORY
Oak Ridge, TN 37831-6283
managed by
UT-Battelle LLC
for the
US DEPARTMENT OF ENERGY
under contract DE-AC05-00OR22725

CONTENTS

LIST OF FIGURES

LIST OF TABLES

ABBREVIATIONS

ATF accident-tolerant fuel

BA burnable absorber

BOC beginning of cycle

BOL beginning of life

BWR boiling water reactor

CBC critical boron concentration

CSV comma separated values

DOE US Department of Energy

DOM Dominant Zone

EOC end of cycle

EOL end of life

HBU high burnup

HFIR High Flux Isotope Reactor

IFBA Integral Fuel Burnable Absorber

LEU low-enriched uranium

LEU+ low-enriched uranium plus

LWR light water reactor

MOC middle of cycle

MOT metaheuristic optimization tool

NRC Nuclear Regulatory Commission

NSGA nondominated sorting genetic algorithm

ORNL Oak Ridge National Laboratory

OSTI Office of Scientific and Technical Information

PPF pin peaking factor

PWR pressurized water reactor

WABA Wet Annular Burnable Absorber

ABSTRACT

Commercial light water reactor (LWR) operators and fuel vendors in the United States are exploring potential changes to nuclear fuel that include low-enriched uranium plus (LEU+) designs to further improve operational economics (e.g., extend cycle length). LEU+ fuel is fuel with a maximum enrichment between 5 wt% and 10 wt% ^{235}U; it allows for higher assembly burnup but likely requires additional reactivity control, e.g., increased burnable absorbers. This report examines possible LEU+ fuel lattice design changes using the lattice physics code, `SCALE/Polaris`. An optimization driver called the Metaheuristic Optimization Tool (MOT) is used to automate domain space exploration and optimization of LEU+ lattice designs. Heuristics from previous LWR lattice optimization studies were used to construct the objective function and define the domain space for optimization. This work successfully demonstrated that the optimization algorithms of MOT can generate feasible, nonproprietary LEU+ lattice designs (GE14 10×10 and Westinghouse 17×17) that meet the constraints of traditional LWR lattices while extending cycle length.

1. INTRODUCTION

As part of the US Nuclear Regulatory Commission (NRC) agreement number 31310019N0008, "SCALE Code Development, Assessment and Maintenance," the effects of low-enriched uranium plus (LEU+), accident-tolerant fuel (ATF), and high burnup (HBU) are being assessed for selected representative light water reactor (LWR) fuel designs. The project is divided into two phases.

Phase 1 focused on identifying the core differences between LEU+ fuel assembly designs and their LEU counterparts. A study investigated lattice physics parameters and used fuel isotopic changes for a conventional GE14 10 $\times$ 10 boiling water reactor (BWR) design with GNF-2 part length rod patterns to model a modern BWR assembly design [2]. Another study within phase 1 investigated the difference between a Westinghouse 17X17 PWR assembly design with LEU with the same assembly design with 8 wt% enriched fuel with 80 GWd/MTHM burnup [3]. Finally, the impact of higher-enrichment (> 5%) ATF fuel designs, namely coated cladding, doped UO_2, and FeCrAl cladding, has been investigated [4]. The phase 1 reports are currently available via US Department of Energy (DOE) Office of Scientific and Technical Information (OSTI).

The present phase 2 report focuses on the automated optimization of LEU+ lattice designs for the GE14 10 $\times$ 10 BWR assembly design and the Westinghouse 17 $\times$ 17 PWR assembly design. The optimization workflow explores the design constraints to optimize the target metrics and inform the feasibility and performance of the LEU+ lattice designs.

2. LATTICE OPTIMIZATION BACKGROUND

Nuclear fuel assemblies have excess reactivity in the beginning of life (BOL) to achieve desired discharge burnups. Typically, initial excess reactivity is suppressed by burnable absorbers (BAs), chemical shims such as soluble boron (not applicable for BWRs), or control rods. The k_{inf} swing in a typical lattice follows an initial increase with BA depletion and a decrease after the peak k_{inf}, which typically occurs around 8–20 GWd/MTHM, depending on the coolant density, type, and concentration of BAs. The goal of lattice optimization performed in this project is to optimize the pin-wise fuel enrichment and BA content in order to minimize excess reactivity, pin peaking factor (PPF), and to maximize fuel cycle length. This work did not investigate the effects of any geometry changes.

Lattice optimization is a challenging design problem because of its large design space, nonlinear response surface, and wide range of conflicting constraints. For example, the GE14 10×10 assembly [5, 6] has 51 unique pins after accounting for diagonal symmetry (Figure 1). Because two parameters can be modified for each pin, when using fuel pin enrichment and Gd concentration without any heuristics, the search yields $51 \times 2 = 102$ continuous variables. Brute force optimization would require an exhaustive search of the 102-dimensional hypercube, which is intractable. Additionally, the response surfaces of many constraints will be not continuous; increasing the enrichment or increasing the Gd concentration of one pin might shift the location of maximum PPF. Multiple objectives mean that there is also complexity—improving one may degrade another. For example, if the objective is to maximize cycle length, then the fuel enrichment in all pins would be maximized. However, another objective is to minimize k_{inf} swing and PPFs, which will lead to trade-offs with the cycle length objective.

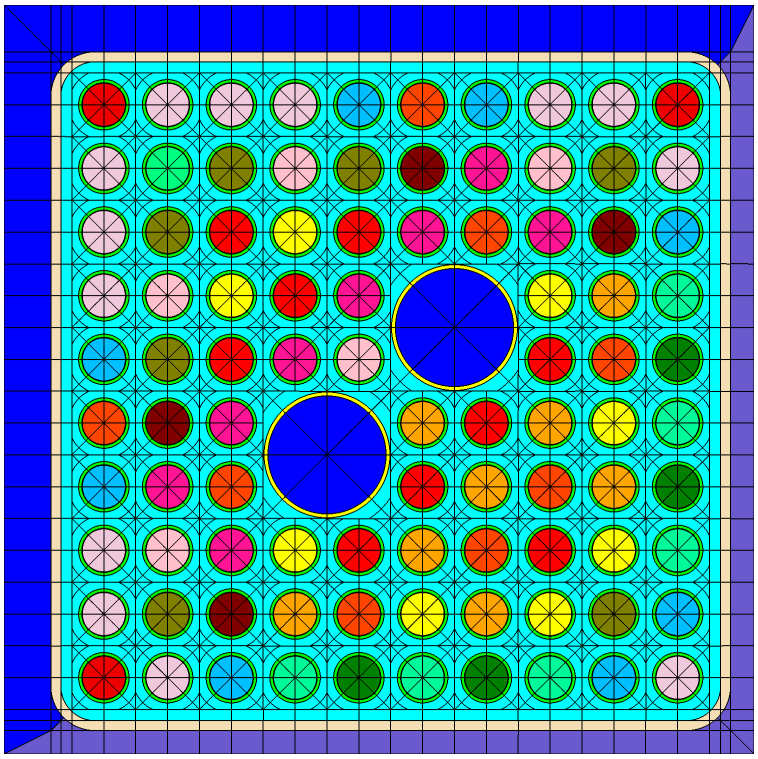

Figure 1. `Polaris`-plotted lattice geometry of GE14 10×10 assembly.

2.1 Survey of BWR Lattice Constraints and Heuristics

To formulate a realistic optimized lattice design, a survey of constraints and heuristics was performed to gather data on what is acceptable and what is "optimal." The survey was performed for low-enriched uranium (LEU) BWR lattice designs. Constraints are important in defining the objective function to guide the optimization algorithm and to search for the correct metrics. Heuristics are important in reducing the design space to "help" the algorithm by providing it with prior knowledge or design best practices, which greatly increases the optimization speed. Applying heuristics to reduce design space might limit novel solutions, so only very well-established heuristics were applied in this work.

Previous studies on BWR lattice optimization [7, 8, 9, 10] focused on similar metrics: BOC k_{inf}, maximum k_{inf}, and maximum PPF. They also used simple heuristics to shape the design space for the optimization problem.

Studies on PWR lattice optimization are not presented because PWR lattices have a smaller, less sensitive design space, and this report focuses primarily on BWR lattice optimization, because it's a more challenging problem.

2.1.1 Constraints

Constraints for a BWR lattice optimization generally include BOC k_{inf}, maximum k_{inf}, and maximum PPF. The specific constraint values used in previous studies are shown in Table 1. As an example, an objective function used in Castillo et al. [7] is shown in Eq. (1). This example discourages lattice average enrichment, high PPF, and deviation from the objective gadolinia concentration and lattice k_{inf}. The importance of a constraint is then dictated by the weighting factor, in which a relatively high weighting factor will cause the value of the objective function to sharply increase when there is a violation of a particular constraint.

$$\begin{aligned} \textit{Minimize} \quad F =& C + W_E E + W_g |G - G_{\text{objective}}| \\ &+ W_p (LPPF_{\max} - LPPF_{\text{limit}}) \\ &+ W_k (k_{\text{inf}} - k_{\text{inf}_{\text{objective}}})^2 \end{aligned} \tag{1}$$

where,

$$\begin{aligned} C &= 50 \\ W &= \text{weighting factor for each metric} \\ E &= \text{lattice-average enrichment} \\ G &= \text{lattice-average gadolinia concentration} \\ LPPF &= \text{local power-peaking factor} \\ k_{inf} &= \text{lattice } k_{inf} \end{aligned}$$

Although optimization should find the minimum irrespective of a constant, C, it is convenient to set the scale to avoid negative values and limit the maximum difference between worst and best solutions.

Table 1. Constraint values used in previous studies.

Authors	Ref.	BOC k_{inf}	Max. k_{inf}	Max. PPF
Radaideh et al.	[10]	-	1.11	1.4 or 1.6
Ortiz-Servin et al.	[9]	1.014–1.017	-	-
Martin-del-Campo et al.	[8]	1.02996	-	1.435
Castillo et al.	[7]	1.0437	-	1.424

2.1.2 Heuristics

The heuristics applied from the literature can be summarized as follows.

1. Gadolinium is not loaded into peripheral (i.e., edge) pins.
2. The lowest enrichment is in the corner pins.
3. Relatively lower enrichment is in the peripheral (i.e., edge) pins.
4. The water rod regions are fixed.

Additionally, the studies sample from a discrete set of enrichment-BA combinations (e.g., 4.4% ^{235}U and 5 wt % gadolinia) to reduce the design space. However, even with 10 discrete fuel composition combinations, there are 10^{51} combinations. Adding the aforementioned heuristics and only assigning lower enrichment pins to edge pins can further reduce the number of combinations but not to a reasonable level that can be optimized by "brute force" in which all combinations are sampled to find an optimal design.

2.2 Boiling Water Reactor Lattice Survey

For additional metrics for an optimized BWR lattice, such as k_{inf} trends and Gd rod locations, a survey of a repository of anonymized few-group cross section data (`t16` files) available at Oak Ridge National Laboratory (ORNL) was conducted. Using the developed data analysis tool, lattice physics characteristics of unrodded dominant region DOM lattices with void fractions at nominal value (40–45%) were evaluated. For this study, only uncontrolled dominant lattice metrics at 45% void fraction were used.

The distribution of BOC, maximum, and EOC k_{inf} values of the DOM lattices are shown in Figure 2. EOC k_{inf} values are evaluated at a 30 GWd/MTHM burnup. Average BOC, maximum, and EOC k_{inf} values are 1.0194, 1.1449, and 1.0627, respectively (N = 25). Figure 3 shows the distribution of the maximum PPFs. The average PPF for the lattice designs is 1.3789. These average values and maximum values demonstrate the expected range of values from the new LEU+ designs.

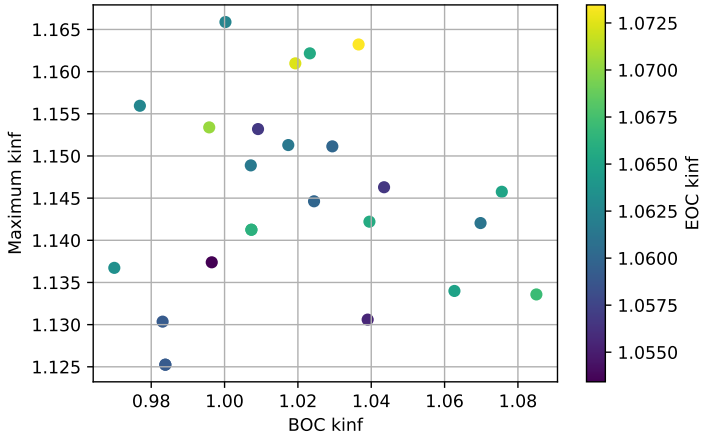

Figure 2. Distribution of BOC and EOC k_{inf} values for uncontrolled DOM BWR lattices.

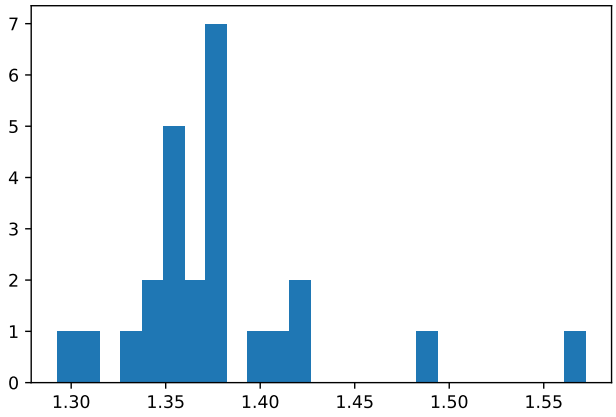

Figure 3. Distribution of maximum PPF for the set of BWR lattice designs.

3. DESIGN DATA AND METHODOLOGY

3.1 Nominal Lattice Design

Two nominal lattice designs were chosen for the optimization study: GE14 10 × 10 BWR and Westinghouse 17 × 17 PWR lattice.

A nominal GE14 10 × 10 BWR lattice was modeled in `Polaris` from a reference design document [11]. Table 2 shows the dimensions of the lattice design. The pin enrichment and Gd_2O_3 concentration are not shown because they are variables to be modified for the optimization study.

A representative Westinghouse 17 × 17 PWR lattice with 200 IFBA pins (Figure 4) was designed at

Table 2. GE14 BWR fuel lattice modeling parameters.

Parameters	Value	Ref.
Lattice size	10×10	
Assembly pitch	15.24 cm	[11]
Fuel rod pitch	1.295 cm	[11]
UO_2 pellet radius	0.4380 cm	[11]
Clad inner radius	0.4470 cm	[11]
Clad outer radius	0.5130 cm	[11]
Water tube inner radius	1.20 cm	[11]
Water tube outer radius	1.28 cm	[11]
Channel width (inside)	13.406 cm	[11]
Channel box thickness	0.2032 cm	[12]
Channel radius	0.9652 cm	[2]
Fuel temperature	900 K	
Cladding temperature	700 K	
Coolant temperature	561.4 K	
Coolant density	0.4214 g/cm^3	

nominal conditions. A uniform fuel enrichment was set as 4.95 wt % for the reference design [1]. Fuel lattice dimensions are shown in Table 3.

Table 3. Westinghouse 17×17 PWR fuel lattice modeling parameters from Sanders and Wagner [1].

Parameters	Value
Lattice size	17×17
Number of fuel rods	264
Number of guide tube	24
Number of instrumentation tube	1
Fuel assembly pitch	21.50 cm
Cell pitch	1.260 cm
Fuel rod diameter	0.8192 cm
Cladding material	ZIRLO
Cladding thickness	0.057 cm
Fuel temperature	800 K
Coolant temperature	550 K
Coolant boron concentration	600 ppm

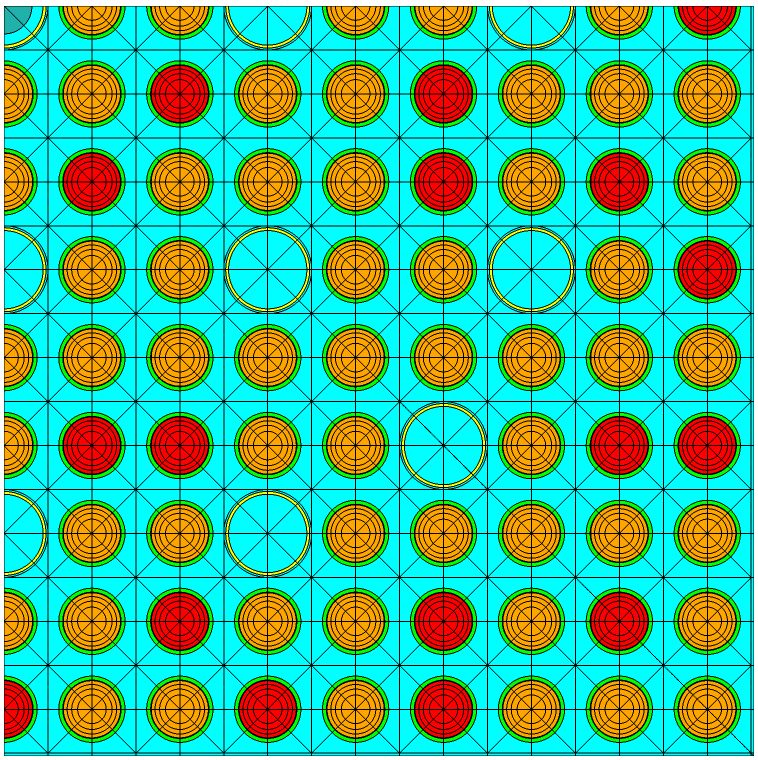

Figure 4. `Polaris`-plotted lattice geometry of a Westinghouse 17 × 17 200 IFBA pin assembly (southeast quarter). The orange pins are IFBA pins, and the red pins are regular UO_2 pins. The hollow cylinders are guide tubes, and the instrumentation tube is located in the upper left corner (center of assembly).

3.2 `SCALE/Polaris` Lattice Physics Code

`Polaris` lattice physics sequence [13] offers novel lattice physics methods and an LWR-analysis focused input interface for lattice physics calculations under SCALE code suit. `Polaris` generates the lattice averaged few-group cross sections (`t16` files) that are used by the PARCS core simulation code. SCALE 56-group ENDF/B-VII.1 cross sections were used in all Polaris calculations in this study to generate optimization metrics, such as k_{inf} and pin peaking factors. `Polaris` was developed with the specific purpose of LWR lattice calculations, with LWR-focused convenient input formatting and optimized calculations, which makes it suitable for the simulation tool for an optimization study.

3.3 Metaheuristic Optimization Tool

MOT [14] is a general optimization and sampling driver code initially developed at ORNL to optimize High Flux Isotope Reactor (HFIR) fuel design parameters. It consists of three primary Python classes collected in the Python `MOT` package: `Perturber`, `Fitter`, and `Method`.

The manner in which the objects are connected when performing an optimization is shown in Figure 5. Users define the optimization problem by describing each search variable in `Perturber` (i.e., parameters

and their ranges) and providing user-defined `Simulation` (i.e., computational process to produce output) and `Function` (i.e., computational process to extract and process the output, such as to read output file and search for a specific result) definitions into `Fitter`. Then, users can insert the initial parameters (i.e., setup) into `Perturber` and `Fitter` classes, which subsequently feed into the `Method` class. Finally, `Method` solves the optimization problem or runs the set of samples described by `Perturber` and `Fitter`. In other words, `Method` governs what the `Perturber` sends to the `Fitter`, and based on what `Method` receives from `Fitter`, it sends new values to the `Perturber` until a user-defined exit condition is met.

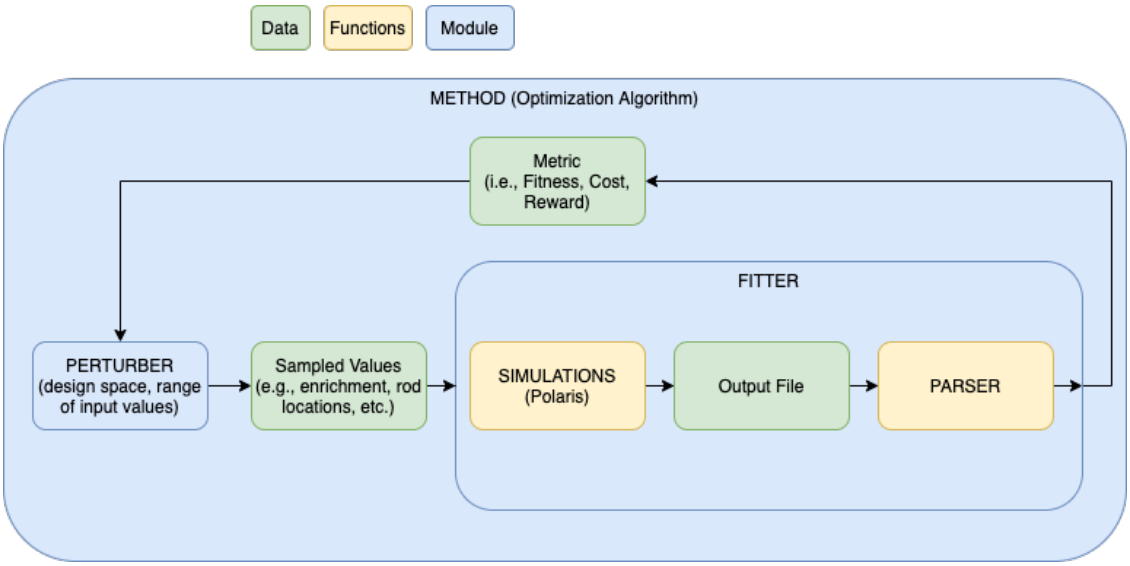

Figure 5. Flowchart of MOT communication between modules.

In this work, `Perturber` contained the design space and possible enrichment values and Gd_2O_3 concentration values for pins in the lattice design. `Fitter` contained functions to create the `Polaris` input file by running the `Polaris` input and parsing the metrics, which are passed to the `Method` class. `MOT` can use many different optimization algorithms, such as simulated annealing and genetic algorithms. Upon preliminary testing, the authors chose the nondominated sorting genetic algorithm (NSGA)-II [15], a genetic algorithm, as the driver for the optimization study. Details of the algorithm and its implementation are provided in the next section.

MOT puts all evaluations of cases into a summary comma separated values (CSV) file in real time. This CSV file can be directly imported into Python as a Pandas [16] data frame for processing and visualization.

3.4 NSGA-II Optimization Algorithm

The chosen optimization algorithm depends on the shape of the response space and the number of parameters. For a smooth response surface, traditional optimization methods that use derivatives or approximations of derivatives can be used. For many dimensions with a well-behaved response surface,

simulated annealing can be used.* However, because the response surfaces for the metrics are discontinuous (e.g., maximum pin-peaking factor, since the location of the pin with the highest peaking factor can change), a genetic algorithm was chosen. Additionally, genetic algorithms are more suitable for parallelization because a set of candidate designs are evaluated every optimization iteration. The optimization algorithm used for this work was NSGA-II [15].

The genetic optimization algorithm is a method for solving an optimization problem based on a natural process that mimics biological evolution. The algorithm takes an initial random set of candidate designs, then modifies them given its fitness (i.e., metric). It takes the better performing candidate designs and uses it to create the next generation through crossover and random mutation. *Crossover* is when certain features that are considered to yield good fitness are taken from a candidate design to move on to the next generation. *Random mutation* is when a feature of a candidate design in the following generation is randomly perturbed so that a wider parameter space can be explored.

A genetic algorithm is set with two important user-defined parameters: the number of generations and the number of samples per generation. These parameters are called *hyperparameters* to differentiate them from simulation parameters, such as pin enrichment and Gd_2O_3 concentration. For each generation, the user-defined number of samples (i.e., simulations) are run and their metrics are evaluated, and the next generation was created by the optimization algorithm to yield better performing candidate designs (i.e., evolve). In the context of this report, this process can be described in the following steps.

1. Randomly generate N (i.e., samples per generation parameter) `Polaris` input files by sampling from a user-defined range of input parameters.
2. Run `Polaris` on the N files.
3. Postprocess output files from each simulation (i.e., run) to obtain metrics.
4. Initiate the optimization algorithm to evaluate the metrics from each candidate design and generate the next generation of N input files (i.e., candidate designs).
5. Repeat steps for the user-defined number of generations.

3.5 Supporting Python Scripts

To set up the optimization workflow, `Polaris` input generation and output parsing needed to be automated. A set of Python classes was developed to read `t16` files and return metrics, such as maximum PPF and k_{inf} history with burnup. Additionally, the classes can read the `Polaris` input and output files to visualize and calculate pin-wise enrichment, Gd_2O_3 concentration, average enrichment values, and pin-wise burnup values.

*Simulated annealing was originally considered for this work, but simulated annealing was considered to be sensitive to the hyperparameters (e.g., cooldown factor). Thus, to provide a workflow that is expandable to problems with varying complexities and response spaces, a genetic algorithm is chosen.

4. OPTIMIZATION PROBLEM DEFINITION

To enforce the constraints, a single objective function with weighted terms was created to minimize maximum PPF, maximize EOC k_{inf}, and minimize maximum k_{inf}.[†]

This section details the optimization problem and the objective functions used for each problem. There are three optimization problems: (1) BWR lattice design optimization, (2) PWR IFBA location optimization, and (3) PWR WABA optimization.

4.1 Boiling Water Reactors

The objective function for the BWR assembly optimization is shown in Eq. (2).

$$\begin{aligned} \text{Minimize} \quad F = & -2\, k_{\text{EOC}} \\ & -2\, f_\epsilon \\ & +2\, \max(0, PPF_{\text{max}} - 1.4) \\ & +10\, \max(0, k_{\text{max}} - 1.15) \\ & +2\, \left| 1 - \frac{k_{\text{BOC}}}{1.05} \right| \\ & +\ N_{\text{lead}} \end{aligned} \tag{2}$$

where,

$k_{\text{EOC}} =$ k_{inf} at 40 $\frac{\text{GWd}}{\text{MTHM}}$

$f_\epsilon =$ assembly-average enrichment divided by maximum pin enrichment

$PPF_{\text{max}} =$ maximum PPF during lattice lifetime (i.e., $\max(PPF(x, BU))$

$k_{\text{max}} =$ maximum k_{inf} from 0 to 40 $\frac{\text{GWd}}{\text{MTHM}}$

$k_{\text{BOC}} =$ k_{inf} of fresh lattice

$N_{\text{lead}} =$ number of statepoints (out of 13 maximum) in which a corner pin has the maximum power

The EOC k_{inf} is evaluated at 40 $\frac{\text{GWd}}{\text{MTHM}}$ to save computational time but also to ensure that the Gd_2O_3 is completely burned off (i.e., the lattice is past its maximum k_{inf}). This objective term essentially functions as a maximizer for discharge burnup without having to deplete the assembly to discharge. There are 13 statepoints up to 40 $\frac{\text{GWd}}{\text{MTHM}}$ for each `Polaris` run. The 13 statepoints are selected through a separate sensitivity study to optimize for runtime, while minimizing loss in fidelity. A compromised fidelity is necessary for the optimization study to proceed in a reasonable time, since there are hundreds of `Polaris` runs in an optimization study. In the end of the optimization study, however, a high fidelity `Polaris` run

[†]Initially, the problem was set up as a multiobjective optimization problem. However, because of the algorithm's tendency to find pareto fronts, it was difficult to force constraints. For example, the algorithm will consider a design with very high maximum k_{inf} as optimal if it had a higher EOC k_{inf} than the other designs. This caused the designs to evolve into having no BAs.

with a finer depletion step resolution is run for the selected design to confirm the validity of the calculation. The f_ϵ term rewards assemblies with maximum and average enrichment that are closer.

The next terms use the max or absolute value to guide the optimization to preferred phase space. The $PPF_{\max}$ term penalizes any $PPF_{\max}$ over 1.4 but does not reward lower values. Similarly, the $k_{\max}$ term penalizes any $k_{\inf}$ above 1.15 but does not reward lower values. The BOC $k_{\inf}$ term encourages values close to 1.05, but values slightly over or under are equally acceptable.

Finally, the N_{lead} term penalizes designs with corner pins having the maximum power. This is related to increased uncertainty in the power at these pins due to, for example, higher influence of moderator density and thus local density/void conditions.

For BWRs, five LEU+ lattices with maximum enrichment values of 6, 7, 8, 9, and 10 were investigated. Heuristics were applied to constrain the prohibitively large design space to a reasonable space for the algorithm to explore. The following heuristics and simplifications were applied.

- Enrichment values can only be multiples of 0.4, except for maximum enrichment value.
- Gd_2O_3 concentration values can only be integer values of 4, 6, and 8.
- Fifty-one unique pins are grouped into 10 enrichment groups based on their location and expert judgement.
- Edge pins cannot have Gd_2O_3.
- Minimum enrichment is 2.0%, and the northwest corner pin can have enrichments down to 0.8%.

4.2 Pressurized Water Reactors

For PWRs, effort focused on designing LEU+ Westinghouse 17×17 lattices with BAs. The study considered two design problems for the optimization demonstration: IFBA location optimization and WABA replacement with Gd_2O_3 and IFBA pins.

Unlike BWR assemblies, PWR assemblies have uniform pin enrichment. Therefore, the design parameter is limited to BA implementation, namely BA location, type, and concentration. BAs' primary roles are to control the initial reactivity of the fresh fuel assembly to prolong its reactivity, control local pin-power peaking, and reduce critical boron concentration (CBC). Suppressing the initial reactivity is more challenging with LEU+ fuel.

Three types of BAs were considered in this report: IFBAs, WABAs, and Gd_2O_3 pins.

- IFBA pins are regular UO_2 pins with a thin layer of ZrB_2. Because of the small quantity of boron, IFBA pins introduce a relatively small reactivity suppression and deplete quicker than the other BAs.
- WABA assemblies are discrete BA components that contain Al_2O_3 and B_4C, which are inserted through the guide tube and removed after the first cycle. WABA assemblies provide a significant suppression of initial reactivity, deplete through the first cycle, and are withdrawn to avoid excess cycle length penalty. However, because of their large negative reactivity, once they are burned, WABA assemblies tend to introduce higher local PPFs. Additionally, implementing WABA assemblies require additional operational maneuvers and storage of the depleted WABA pins after discharge.

- Gd_2O_3 pins are regular UO_2 pins with Gd_2O_3 integrated into the fuel pin up to 8 wt %. Gadolinium has a significantly higher thermal absorption cross section than boron, so it provides a significant reactivity suppression. However, adding Gd_2O_3 into UO_2 lowers the fuel pin thermal conductivity [17], which is unfavorable. Additionally, Gd_2O_3 pins can introduce higher local PPF later in the cycle. UO_2-Er_2O_3 pins were not investigated in this work.

One notable difference between boron-based BAs and Gd-based BAs is the magnitude of the absorption cross section and transmutation of the BA with burnup. The absorption cross section of natural Gd (Table 4) is several orders of magnitude higher than that of ^{11}B and ^{10}B (Figure 6).

Natural Gd is used for all the designs in this report. Using natural Gd causes an "extended" (relative to boron) reactivity suppression due to the absorption chain of lighter Gd isotopes transmuted to heavier Gd isotopes, which have high-absorption cross sections. This causes natural Gd to be a good BA for initial reactivity suppression, but using it at high concentrations can cause a higher cycle length penalty due to the transmutation of its isotopes at high burnups.

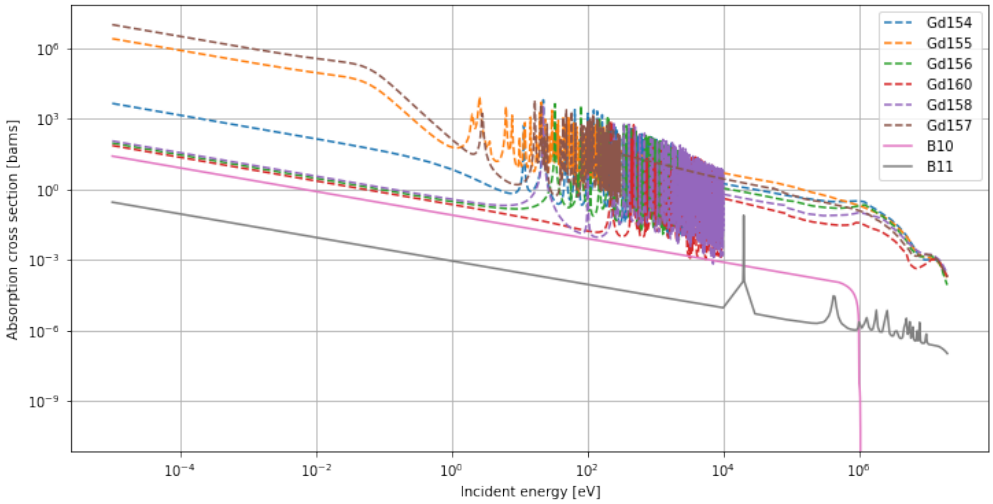

Figure 6. Absorption cross section values of isotopes used in BAs.

Table 4. Gadolinium natural abundance. All isotopes listed are stable, except for ^{152}Gd, which has a half life of ~10^{14} years.

Isotope	Abundance (atom %)
^{152}Gd	0.2
^{154}Gd	2.18
^{155}Gd	14.80
^{157}Gd	15.65
^{156}Gd	20.47
^{158}Gd	24.84
^{160}Gd	21.86

4.2.1 IFBA Optimization Objective Function

The objective function in Eq. (3) was used for IFBA optimization.

$$\begin{aligned} \text{Minimize} \quad F = & - k_{\text{EOC}} \\ & + 1.5\ PPF_{\text{max}} \\ & + 1.5\ k_{\text{max}} \\ & + 2\ \left| \frac{k_{\text{ref}} - k_{\text{BOC}}}{k_{\text{ref}}} \right| \\ & + \max(0, N_{\text{IFBA}} - N_{\text{ref}}) \end{aligned} \tag{3}$$

where,

$$\begin{aligned} k_{\text{EOC}} &= k_{\text{inf}} \text{ at } 30\ \frac{\text{GWd}}{\text{MTHM}} \\ PPF_{\text{max}} &= \text{maximum PPF during lattice lifetime (i.e., } \max(PPF(x, BU)) \\ k_{\text{max}} &= \text{maximum } k_{\text{inf}} \text{ from 0 to } 30\ \frac{\text{GWd}}{\text{MTHM}} \\ k_{\text{BOC}} &= k_{\text{inf}} \text{ of fresh lattice} \\ k_{\text{ref}} &= k_{\text{inf}} \text{ of reference design} \\ N_{\text{IFBA}} &= \text{number of IFBA pins in design} \\ N_{\text{ref}} &= \text{number of IFBA pins in reference design (80, 200)} \end{aligned}$$

The goals were to

- match the reference design's BOC k_{inf},
- minimize the maximum PPFs,
- minimize the maximum k_{inf},
- maximize the EOC k_{inf}, and
- not exceed the number of IFBA pins in the reference design.

4.2.2 WABA Replacement with Integrated Burnable Absorbers with Optimization

As mentioned in Section 4.2, Wet Annular Burnable Absorber (WABA) assemblies are inserted through the guide tube to provide initial excess reactivity suppression in the first cycle. This provides an attractive burnable poison option, but because boron is replaced with water, it also caused high PPFs after the WABA withdrawal. Additionally, implementing WABAs incurs additional operational procedure and waste storage.

For WABA optimization, the objective function in Eq. (4) was used to minimize maximum PPF and maximum k_{inf} while maximizing EOC k_{inf} and achieving a similar k_{inf} curve to the WABA insertion

scenario, as shown in Figure 25. The EOC k_{inf} was evaluated at 40 GWd/MTHM to account for differences in BA usage that affect k_{inf} peaks and slopes.

$$\begin{aligned} \text{Minimize} \quad F = & - k_{\text{BOC}} \\ & + 1.5\ PPF_{\text{max}} \\ & + 1.5\ k_{\text{max}} \\ & + 2\ \left|\frac{1.0078 - k_{\text{BOC}}}{1.0078}\right| \end{aligned} \tag{4}$$

where,

$$\begin{aligned} k_{\text{EOC}} = & \quad k_{\text{inf}} \text{ at } 40\ \frac{\text{GWd}}{\text{MTHM}} \\ PPF_{\text{max}} = & \quad \text{maximum PPF during lattice lifetime (i.e., max}(PPF(x, BU)) \\ k_{\text{max}} = & \quad \text{maximum } k_{\text{inf}} \text{ from 0 to } 40\ \frac{\text{GWd}}{\text{MTHM}} \\ k_{\text{BOC}} = & \quad k_{\text{inf}} \text{ of fresh lattice} \end{aligned}$$

5. RESULTS

The optimization results are organized in two parts: an explanation of the evolutionary process of lattice designs from the design scope and an in-depth explanation of a selected design for each optimization study.

5.1 BWR Lattice Optimization for Varying Maximum Enrichment

Five optimization studies were run for BWR lattice designs for pin maximum enrichment values up to 6, 7, 8, 9, and 10. The objective function is the same for all five optimization runs (Section 4.1), as well as the design space (Section 4.1). The only difference is the maximum enrichment value that the algorithm can perturb. The evolutionary algorithm was run with 96 samples per generation and terminated when none of the candidate designs improve further.

Forty-eight cores were used to execute lattice depletion calculations in parallel. Running one generation of 96 samples takes ~1.64 h.

The initial randomized designs return infeasible lattice designs, but throughout the generation, the lattice designs (i.e., samples) evolve into a more feasible, improved design. Figures 7 to 11 show the evolution of the design metrics with increasing generation. Because maximum PPF and maximum k_{inf} are constrained to not exceed 1.4 and 1.15, respectively, the algorithm stays along the value while trying to maximize average enrichment and EOC k_{inf}. In other words, the scatter plots for BOC k_{inf} and maximum k_{inf} show convergence, whereas plots for EOC k_{inf} and average enrichment move to the right with increasing generation.

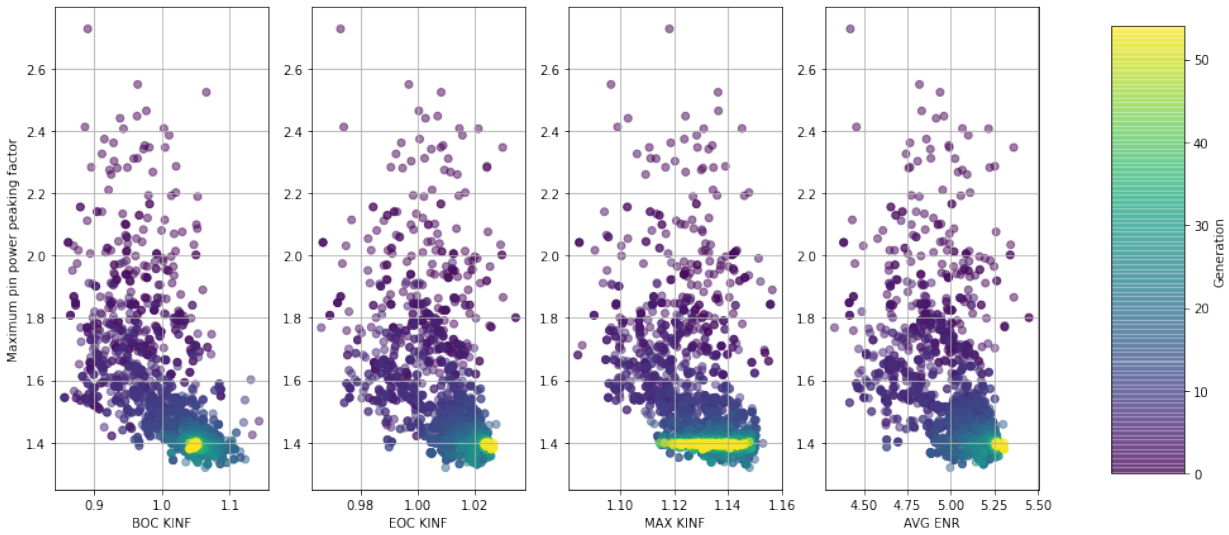

Figure 7. Evolution of NSGA-II–driven optimization of BWR assemblies throughout the evolutionary generation for maximum pin enrichment of 6 wt%. The four metrics evolve to a desired direction with increasing generation.

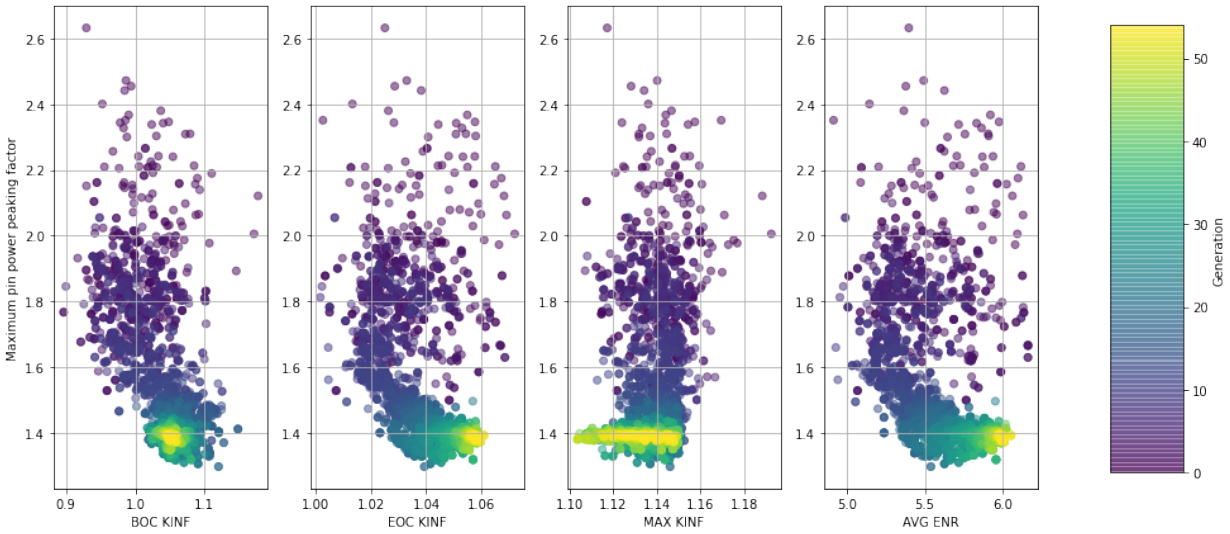

Figure 8. Evolution of NSGA-II–driven optimization of BWR assemblies throughout the evolutionary generation for maximum pin enrichment of 7 wt%. The four metrics evolve to a desired direction with increasing generation.

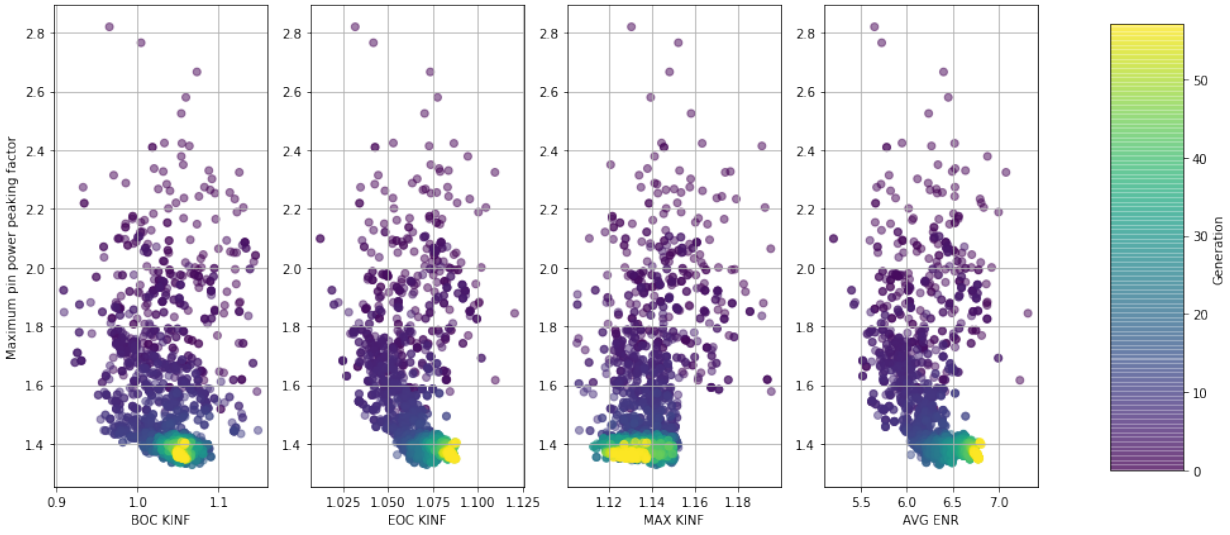

Figure 9. Evolution of NSGA-II–driven optimization of BWR assemblies throughout the evolutionary generation for maximum pin enrichment of 8 wt%. The four metrics evolve to a desired direction with increasing generation.

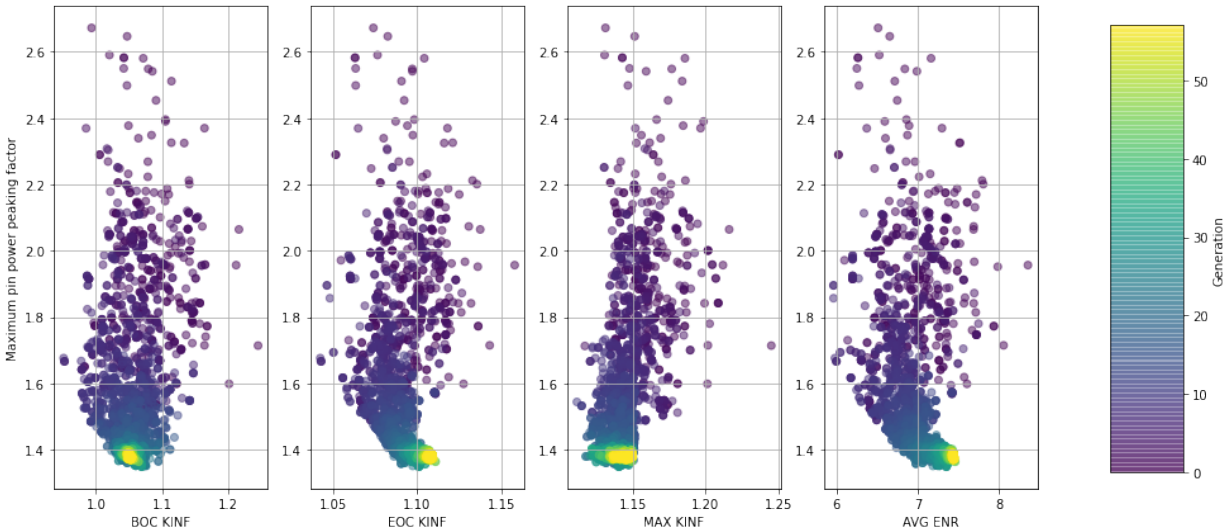

Figure 10. Evolution of NSGA-II–driven optimization of BWR assemblies throughout the evolutionary generation for maximum pin enrichment of 9 wt%. The four metrics evolve to a desired direction with increasing generation.

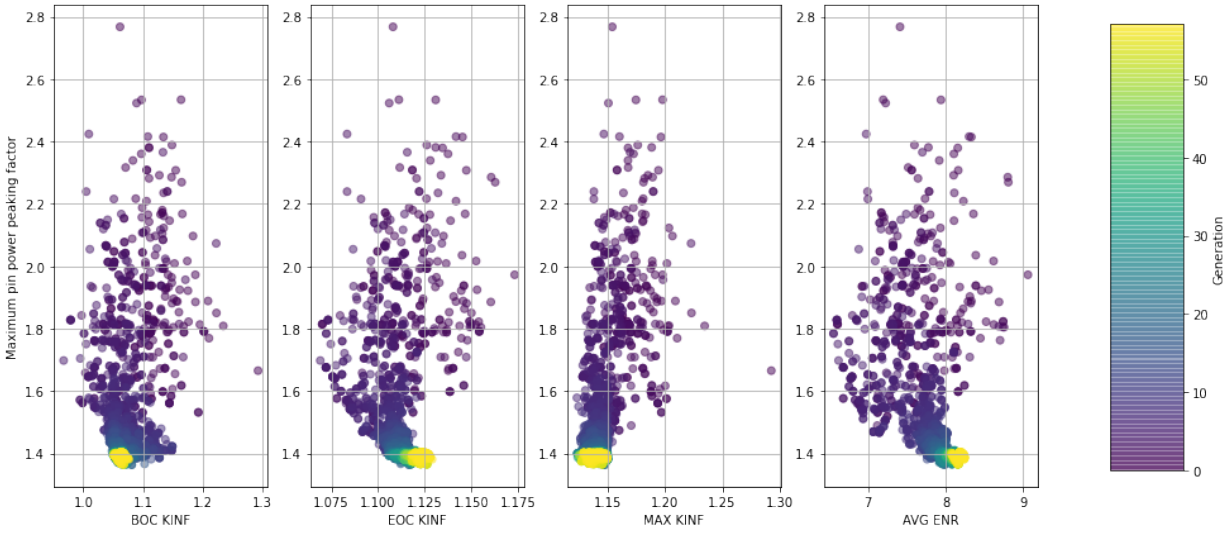

Figure 11. Evolution of NSGA-II–driven optimization of BWR assemblies throughout the evolutionary generation for maximum pin enrichment of 10 wt%. The four metrics evolve to a desired direction with increasing generation.

From all the potential surveyed designs, the following filters were applied to select feasible designs:

1. BOC k_{inf} between 1.03 and 1.05,
2. maximum k_{inf} less than 1.15, and
3. maximum PPF less than 1.4.

The feasible designs found by the optimization algorithm are shown in Figure 12 in which a stratified EOC k_{inf} is shown with maximum pin enrichment. Because of the constraints put on the maximum Gd_2O_3 concentration, fewer feasible designs were found for higher maximum enrichment values. Because the fuel enrichment—and, thus, the initial excess reactivity—is so high, more Gd_2O_3 must be implemented to meet BOC k_{inf} constraints, which later causes higher PPF. In other words, given the very specific k_{inf} range in the first cycle (1.05–1.15), it is more challenging to control the excess reactivity of the higher enriched fuel while meeting PPF limits with burnup.

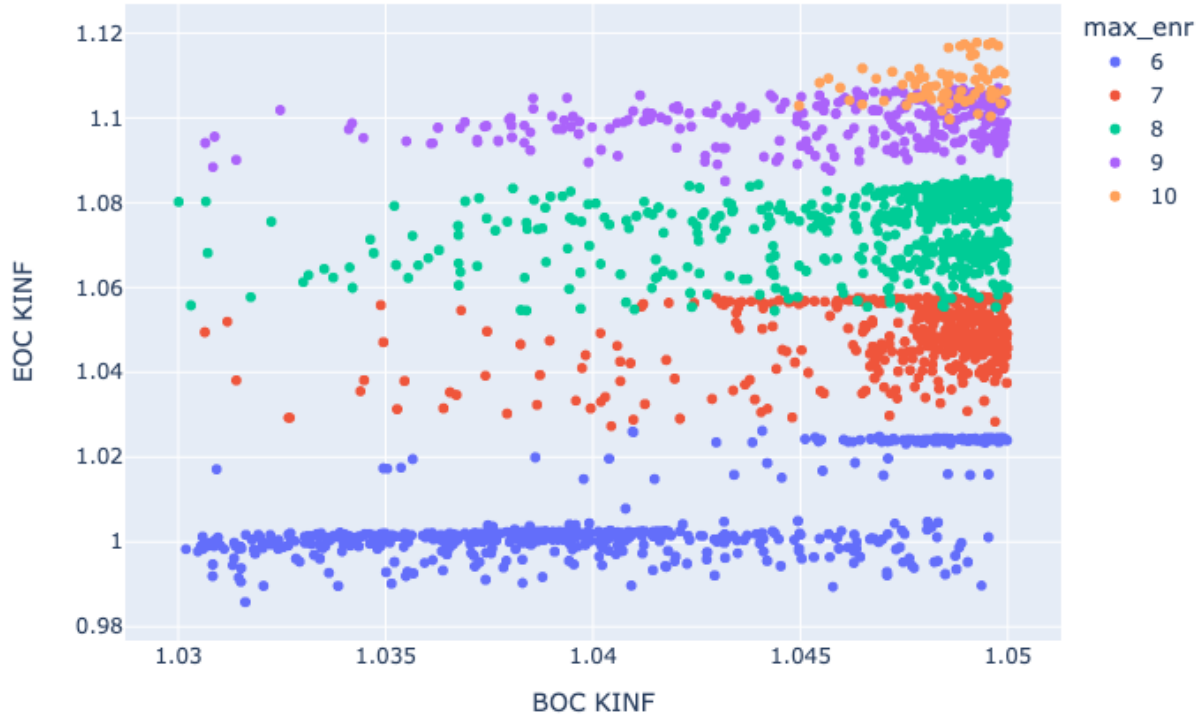

Figure 12. Feasible designs found for maximum enrichments of 6, 7, 8, 9, and 10 for GE14 10 × 10 BWR designs.

For each maximum enrichment, the feasible design with the highest assembly-average enrichment was selected and visualized for comparison (Figure 13). The reactivity curve shape (i.e. the burnup at which maximum k_{inf} occurs) is dependent on the ratio between the assembly enrichment and the BA loading. Most designs show a similar increase of k_{inf} in the first cycle up to 20 GWd/MTHM. The higher

enrichment lattices with higher Gd_2O_3 loading sustain k_{inf}, whereas the lower enrichment lattices start to decrease in k_{inf}. The higher enrichment lattices have higher EOC k_{inf} values. The pin maps for each optimized design are shown in Figures 14 to 18.

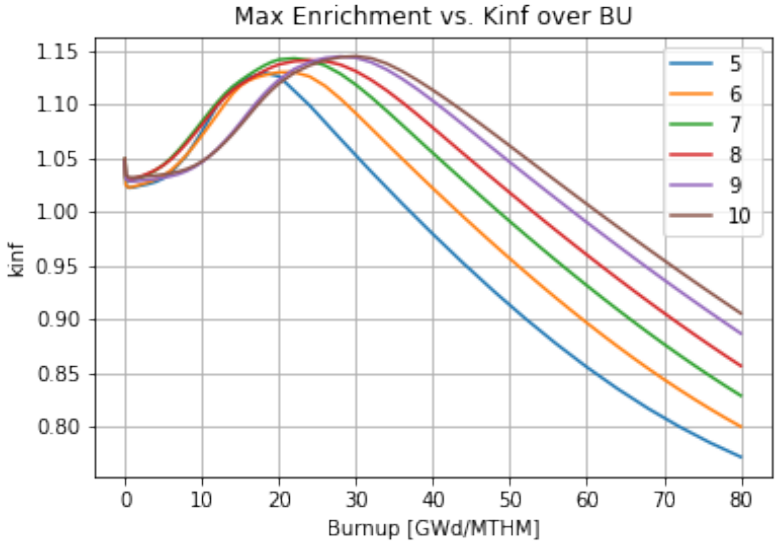

Figure 13. k_{inf} vs. burnup plot for optimized designs for each maximum fuel enrichment constraint.

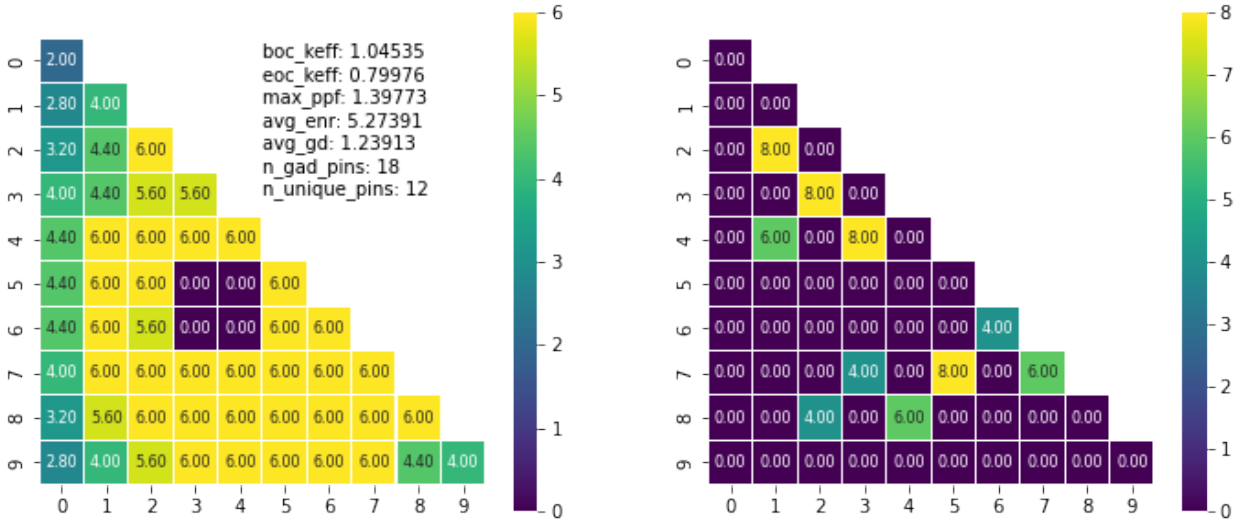

Figure 14. Pin maps of optimized designs for maximum pin enrichment of 6 wt %. The fuel enrichment maps are shown on the left, and the Gd_2O_3 loadings (wt %) are shown on the right.

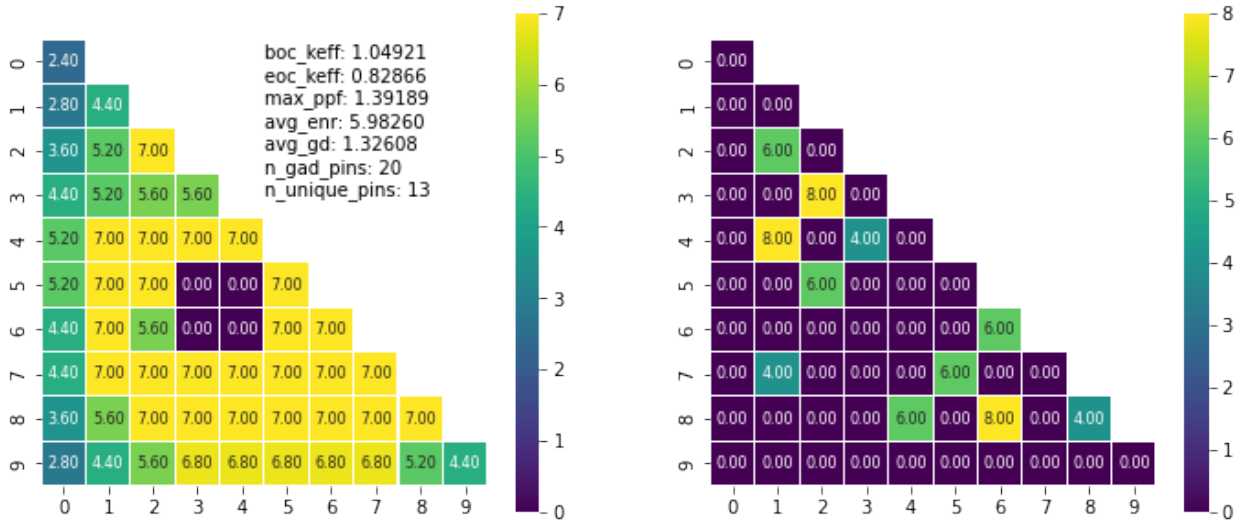

Figure 15. Pin maps of optimized designs for maximum pin enrichment of 7 wt %. The fuel enrichment maps are shown on the left, and the Gd_2O_3 loadings (wt %) are shown on the right.

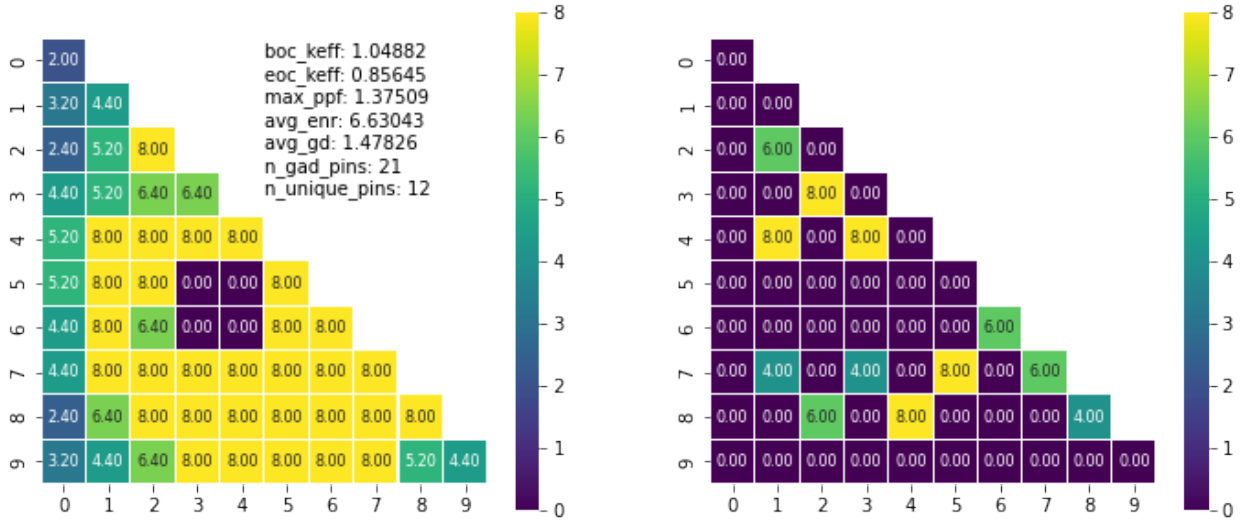

Figure 16. Pin maps of optimized designs for maximum pin enrichment of 8 wt %. The fuel enrichment maps are shown on the left, and the Gd_2O_3 loadings (wt %) are shown on the right.

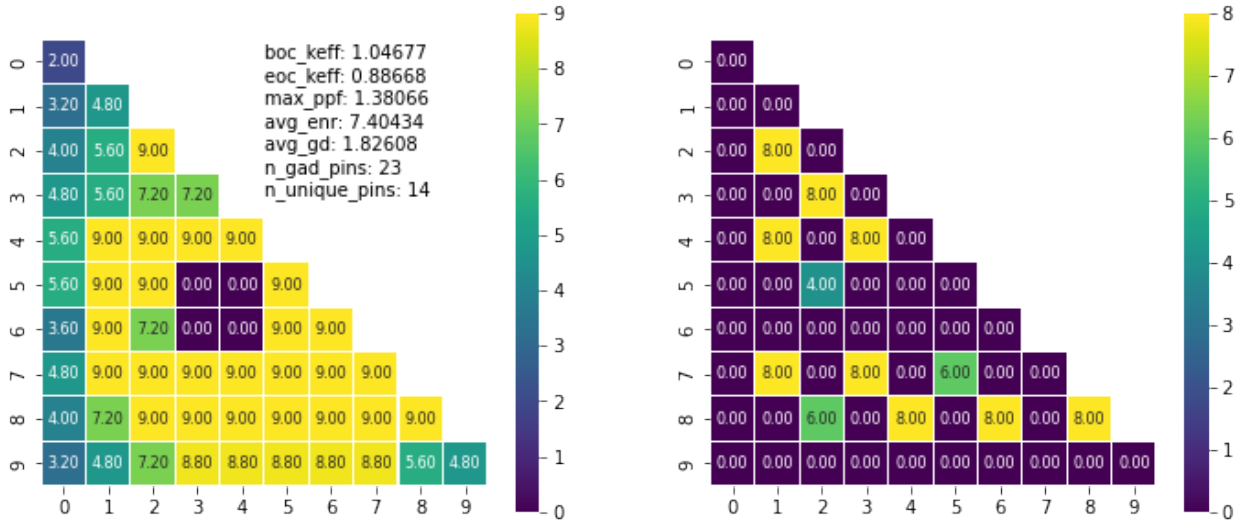

Figure 17. Pin maps of optimized designs for maximum pin enrichment of 9 wt %. The fuel enrichment maps are shown on the left, and the Gd_2O_3 loadings (wt %) are shown on the right.

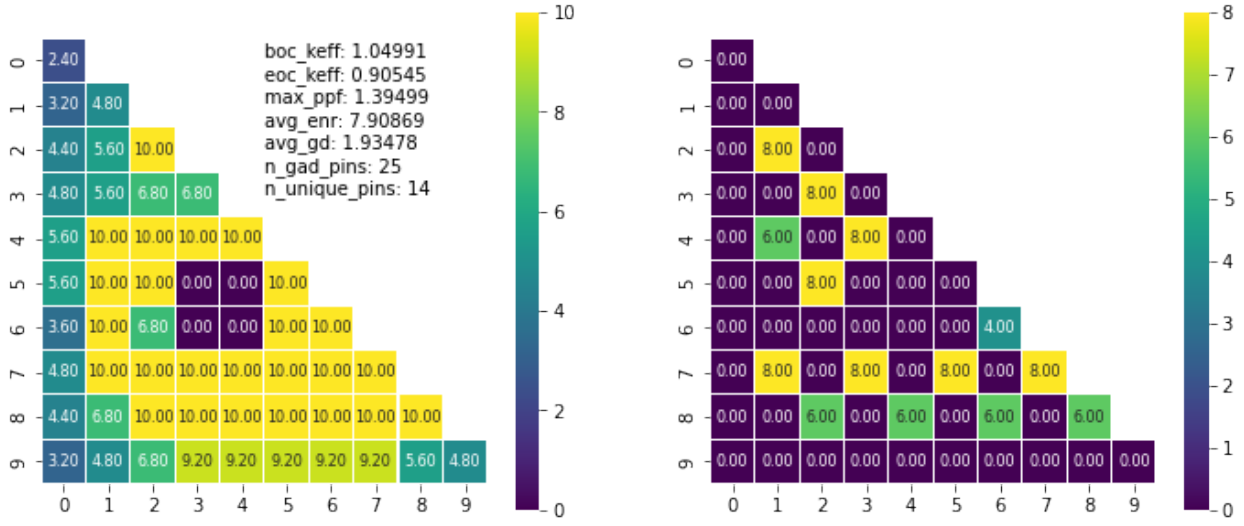

Figure 18. Pin maps of optimized designs for maximum pin enrichment of 10 wt %. The fuel enrichment maps are shown on the left, and the Gd_2O_3 loadings (wt %) are shown on the right.

5.2 PWR IFBA Location Optimization

Two optimization studies for IFBA location optimization were run: one for 200 IFBA pins and one for 80 IFBA pins. A reference design for an 80-IFBA pin design was obtained from Sanders and Wagner [1], and the enrichment was raised to 5.95%. The reference 200-IFBA pin design was obtained from the LEU+ phase II PWR core analysis [18].

The optimization problem was set so that the 39 unique fuel pins in the assembly—accounting for symmetry and guide/instrumentation tubes—can be a regular fuel pin or an IFBA pin. The algorithm could choose between 0 and 1 for each pin location, where 0 denotes a fuel pin, and 1 denotes an IFBA pin. The binary vector was then passed on to create a `Polaris` input with the defined pin map to calculate the k_{inf} curve and the PPFs. The input file also went through a script that calculated the total number of IFBA pins in the assembly given the location of the pins in the pin map.

Thirty-two cores were used to execute lattice depletion calculations in parallel. Running one generation of 96 samples takes ~1.75 h.

Figures 19 and 20 show the evolution of the lattice design metrics for 80 and 200 IFBA pin designs, meaning the maximum number of IFBA pins they can have are 80 and 200, respectively. The objective function causes the designs to reach the IFBA pin numbers to meet the BOC k_{inf} value and then calibrates the IFBA pin locations to minimize PPF and maximum k_{inf}.

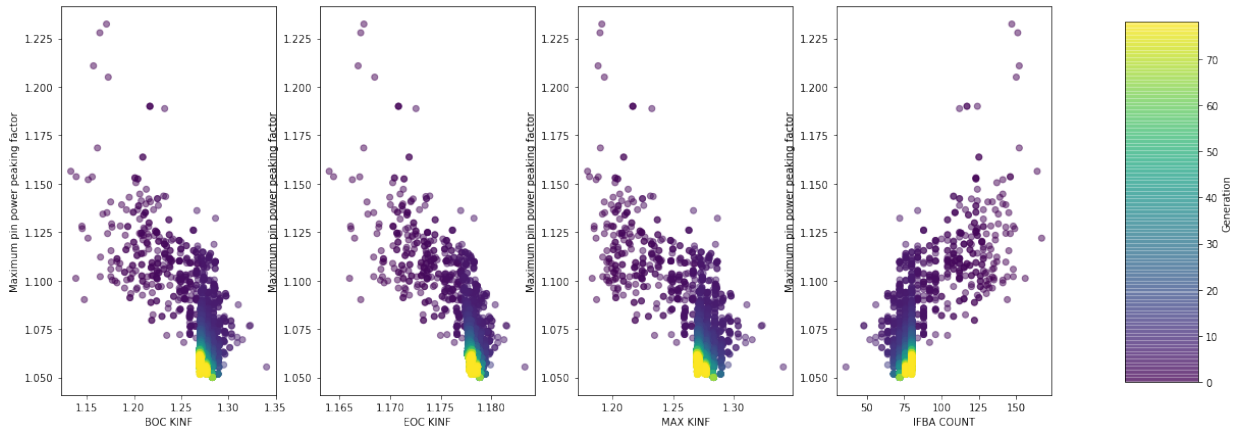

Figure 19. Evolution of IFBA pin location optimization designs. The IFBA count metric is constrained at 80.

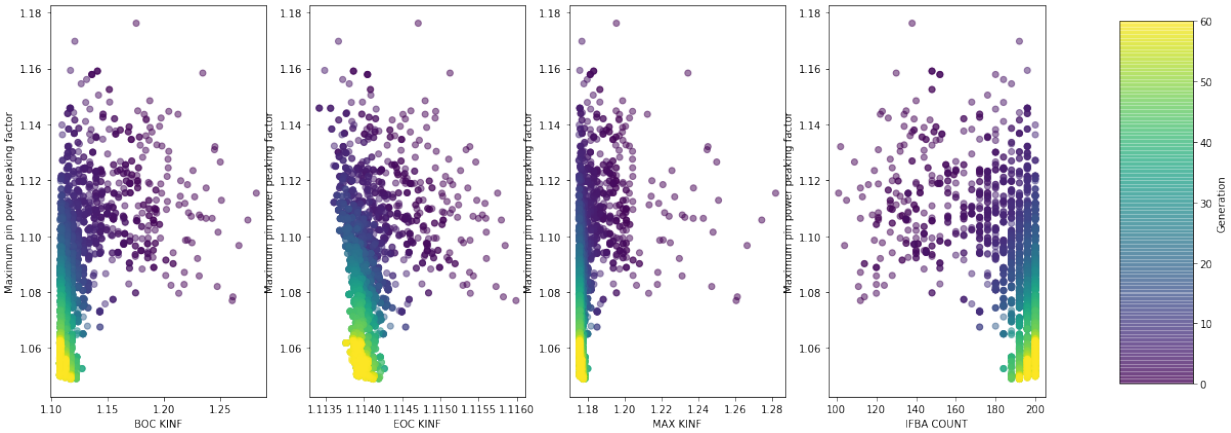

Figure 20. Evolution of IFBA pin location optimization designs. The IFBA count metric is constrained at 200.

From the sampled designs, an optimized design was selected and compared with the reference design (Figure 21). For both designs, there was no difference in the k_{inf} curve because the reference and optimized designs have the same number of IFBA pins and thus the same BA loading. The difference comes from the location of the IFBA pins, and the optimized design showed a lower average maximum PPF curve than the reference design. The optimized design pin maps (Figure 22) show that the algorithm focused the IFBA pins to the center of the assembly to lower the PPF. The local PPF heat maps are shown in Figures 23 and 24. The PPF distribution of the optimized design is more evenly distributed than the reference designs.

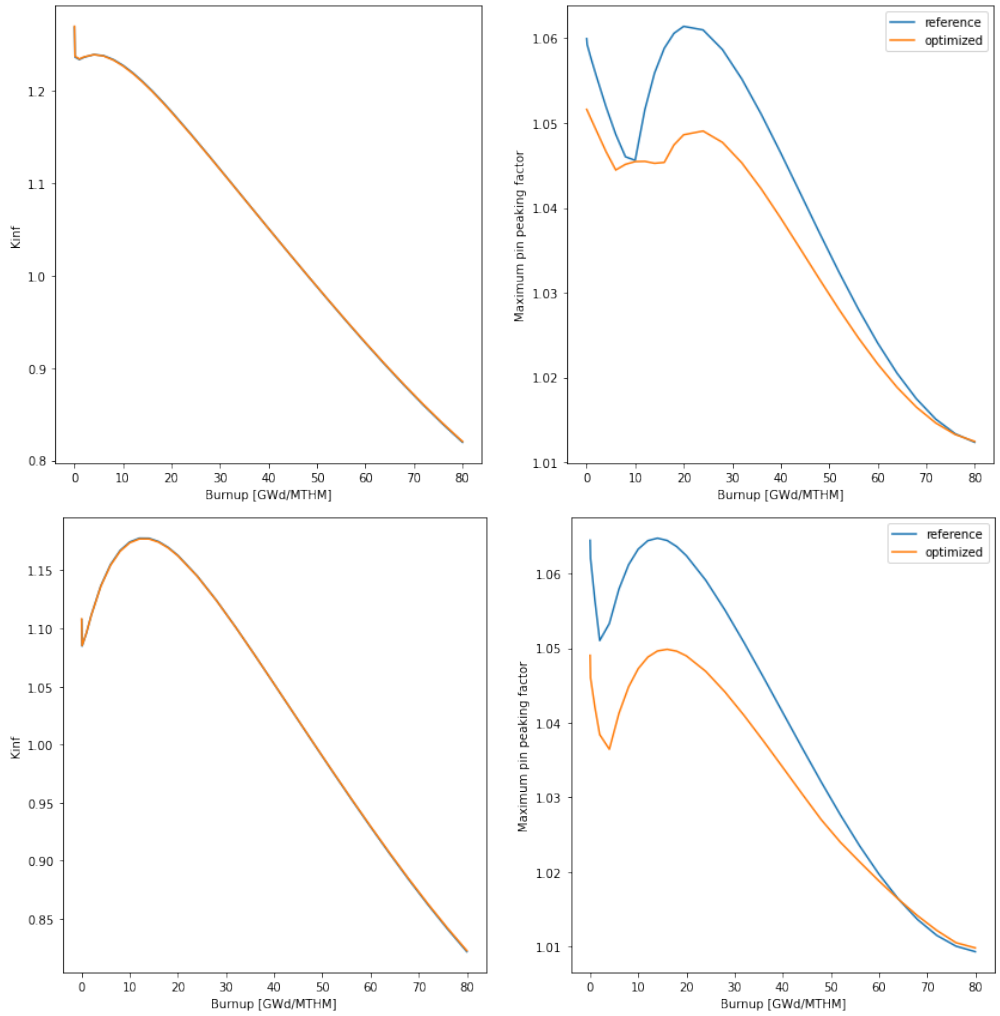

Figure 21. Selected optimized lattice designs for 80 (top) and 200 (bottom) IFBA designs. There are no significant changes in the k_{inf} curve (left) because the number of IFBA pins is the same, but the optimized designs have lower average PPFs (right).

Figure 22. Pin map of the southeast quarter of the full assembly of the reference designs for 80 (top left) and 200 (bottom left) IFBA pin designs compared with the optimized designs for 80 (top right) and 200 (bottom right) IFBA pin designs.

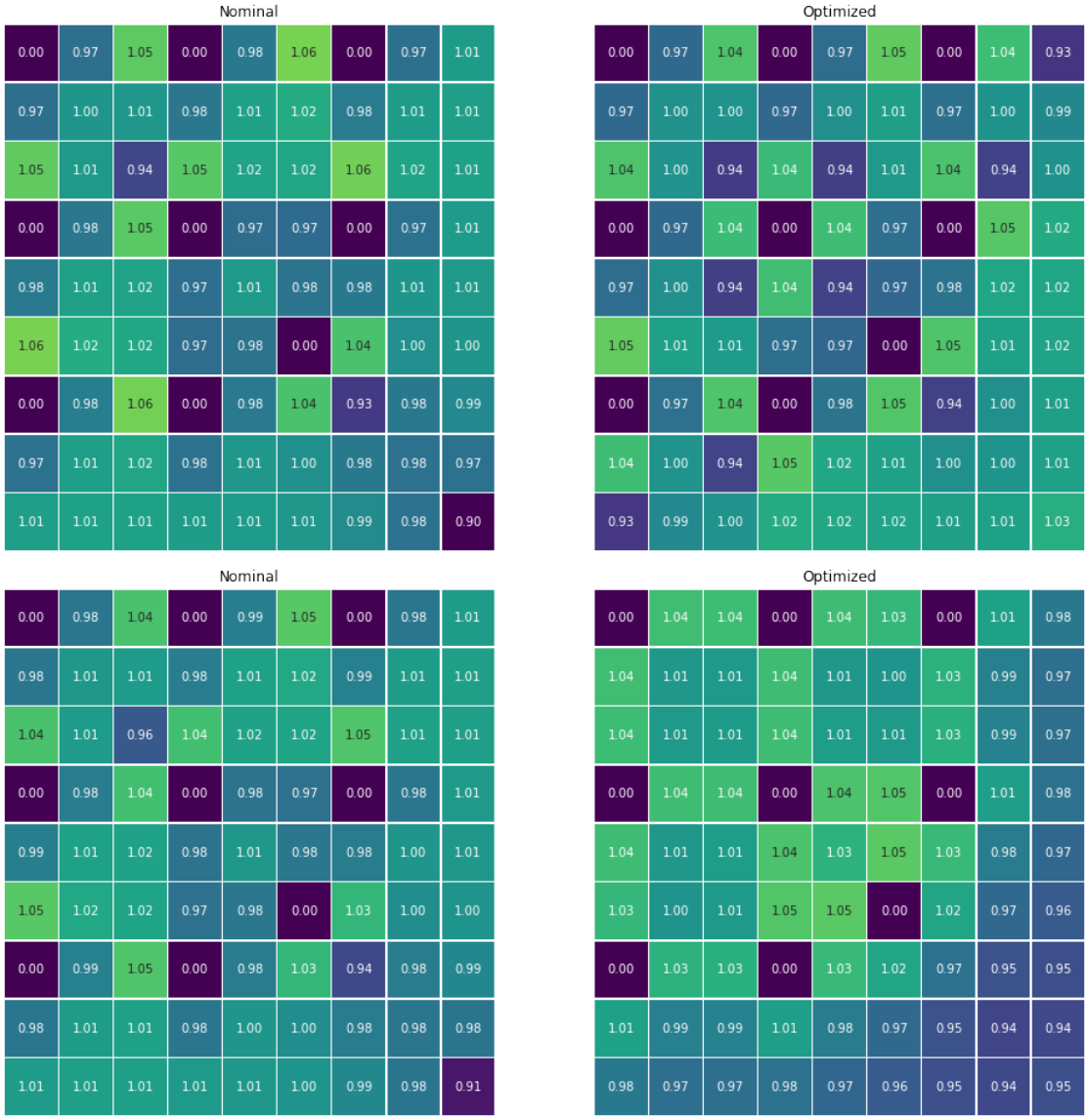

Figure 23. PPF distribution of the 80-IFBA lattice at BOC (top) and at 22 GWd/MTHM (bottom) when peak PPF occurs for the reference design. The reference design is shown on the left, and the optimized design is shown on the right.

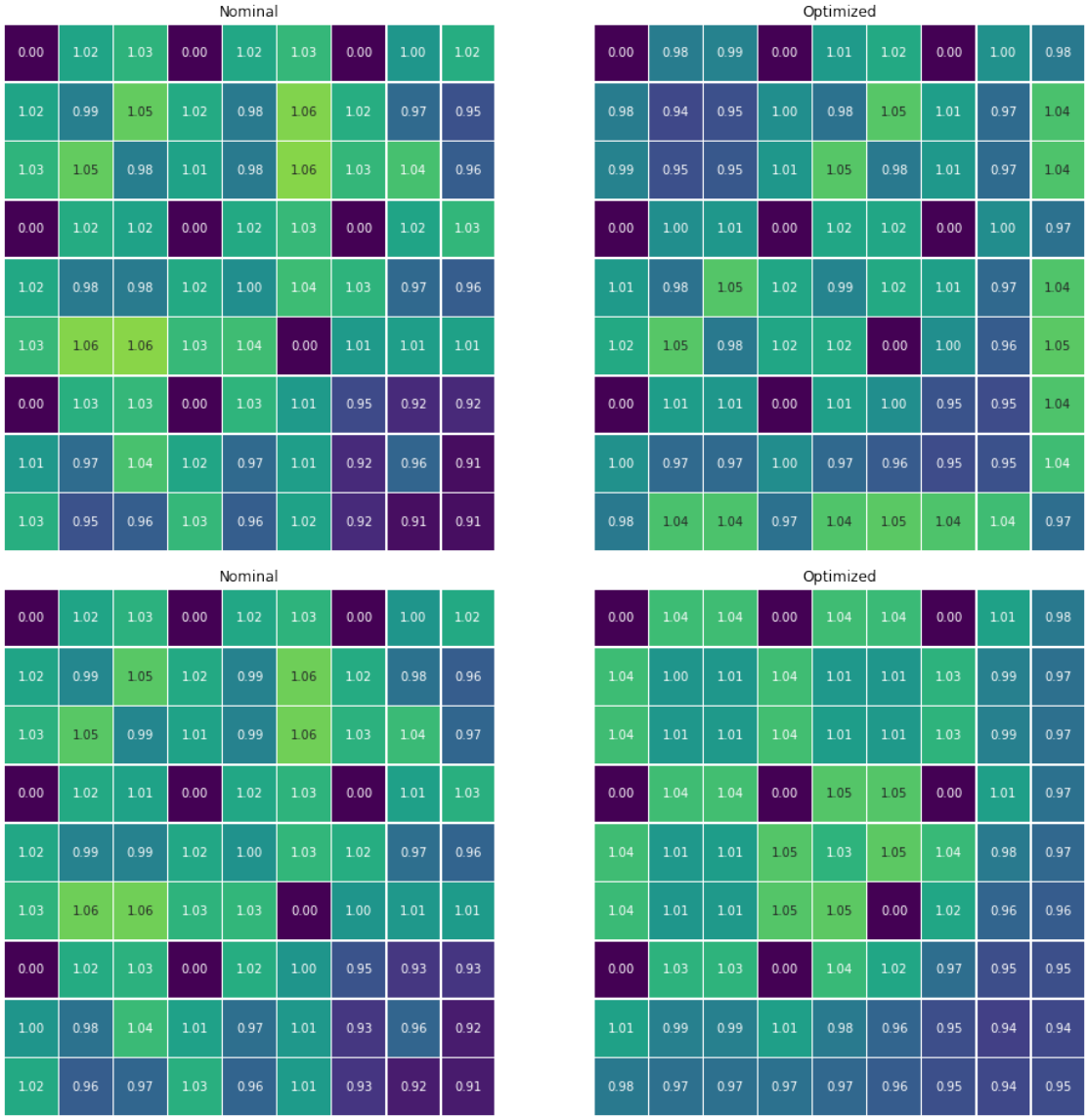

Figure 24. PPF distribution of the 200-IFBA lattice at BOC (top) and at 18 GWd/MTHM (bottom) when peak PPF occurs for the reference design. The reference design is shown on the left, and the optimized design is shown on the right.

5.3 PWR Wet Annular Burnable Absorber Replacement with Hybrid Burnable Absorber

As mentioned in Section 4.2, WABA assemblies were inserted through the guide tube to provide initial excess reactivity suppression in the first cycle. This provided an attractive burnable poison option, but because boron is replaced with water, it also caused high PPFs after WABA was withdrawn. Additionally, implementing WABAs incurred additional operational procedure and waste storage.

This optimization study considered replacing WABA implementation with Gd_2O_3 fuel pins in addition to IFBA pins while obtaining a similar k_{inf} curve with burnup and a lower PPF. A reference design using an enrichment of 5.95% was also used for this study.

A study in which the 200 IFBA lattice was modified to have the choice of three pins—a UO_2 pin, an IFBA pin, and a Gd_2O_3 UO_2 pin—was set up. To simplify the optimization dimension, the Gd_2O_3 concentration was fixed. Four studies were run in which the fixed Gd_2O_3 concentrations were 1, 2, 4, and 6 wt %.

Inserting WABA in the BOC suppressed the initial excess reactivity but also increased the maximum PPF. Notably, the maximum PPF jumped when the WABA was withdrawn because the boron was replaced with water in the lattice (Figure 26). We assume WABA withdrawal at 25 GWd/MTHM, which is approximately the lattice burnup after the first cycle [18]. Achieving a similar k_{inf} curve with the WABA design using Gd_2O_3 pins was difficult because Gd_2O_3 pins have a longer-lasting reactivity penalty due to its natural composition and transmutation chain.

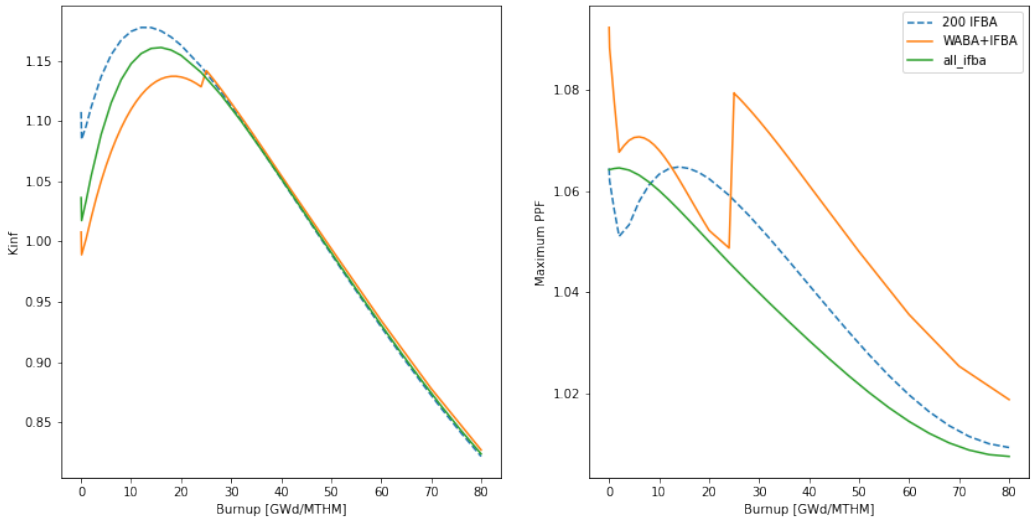

Figure 25. k_{inf} and maximum PPF curve with burnup plot for a reference 200-IFBA pin case and 200-IFBA case with WABA insertion. WABA is pulled out at 25 GWd/MTHM. The 'all_ifba' line refers to a design with all pins being IFBA pins, for comparison.

The different characteristics of BAs create an interesting problem. IFBA pins provide good initial reactivity suppression without causing any longer-term reactivity penalty. However, because IFBA pins contain little boron, the suppression effect burns out at middle of cycle (MOC) (~20 GWd/MTHM). To supplement the

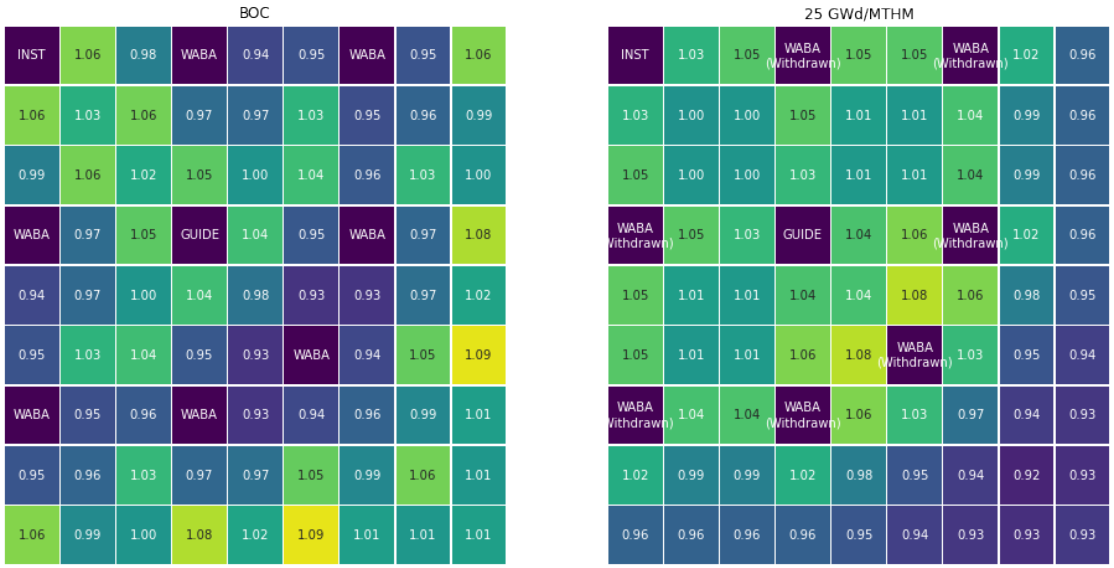

Figure 26. WABA PPF pin map at BOC (left) and 25 GWd/MTHM (right) when WABA is withdrawn. Maximum PPF occurs around the withdrawn WABA positions.

reactivity suppression, Gd_2O_3 pins can be implemented to further reduce reactivity, especially in the MOC. However, implementing Gd_2O_3 pins incurs long-term reactivity penalty.

As expected, the algorithm increased IFBA pin numbers to meet BOC k_{inf} (Figures 27 to 30). The number of Gd_2O_3 pins decreased because implementing Gd_2O_3 pins decreases EOC and increases maximum PPF. The best-performing design was a lattice with four Gd_2O_3 pins (2% concentration) and the remaining IFBA pins. Its EOC k_{inf} was ~2,000 pcm lower than that of the WABA design.

Another exploratory study was performed in which the BOC k_{inf} constraint was relaxed, and the design space was expanded to increase enrichment from 5.95 to 6.8%. The higher enrichment will provide higher EOC k_{inf} and enable more Gd_2O_3 pin implementation to suppress initial excess reactivity. Two candidate designs were selected: (1) one with 6.4% enrichment, four Gd_2O_3 pins (3% concentration), and the remaining IFBA pins and (2) one with 6.8% enrichment, 12 Gd_2O_3 pins (1% concentration), and the remaining IFBA pins (Figure31). The two designs do not meet the BOC k_{inf} constraint but meet the k_{inf} value at 50 GWd/MTHM. The different effects of boron and Gd are shown where the WABA design has more reactivity suppression earlier in the cycle that burns out, whereas designs with Gd_2O_3 pins have a more persistent suppression of reactivity. Selecting a “better” design between the two will depend on the priority of metrics (i.e., less enrichment vs. less excess reactivity).

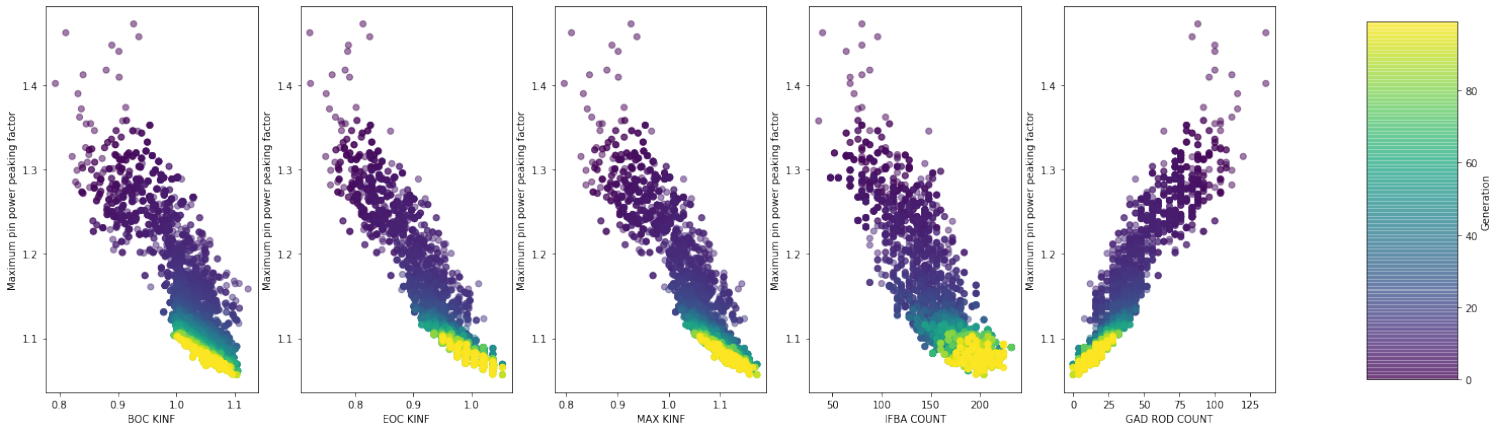

Figure 27. Evolution of NSGA-II–driven optimization of PWR assemblies with 1 wt % Gd_2O_3 pins. The algorithm struggles to increase EOC k_{inf} while keeping BOC in control.

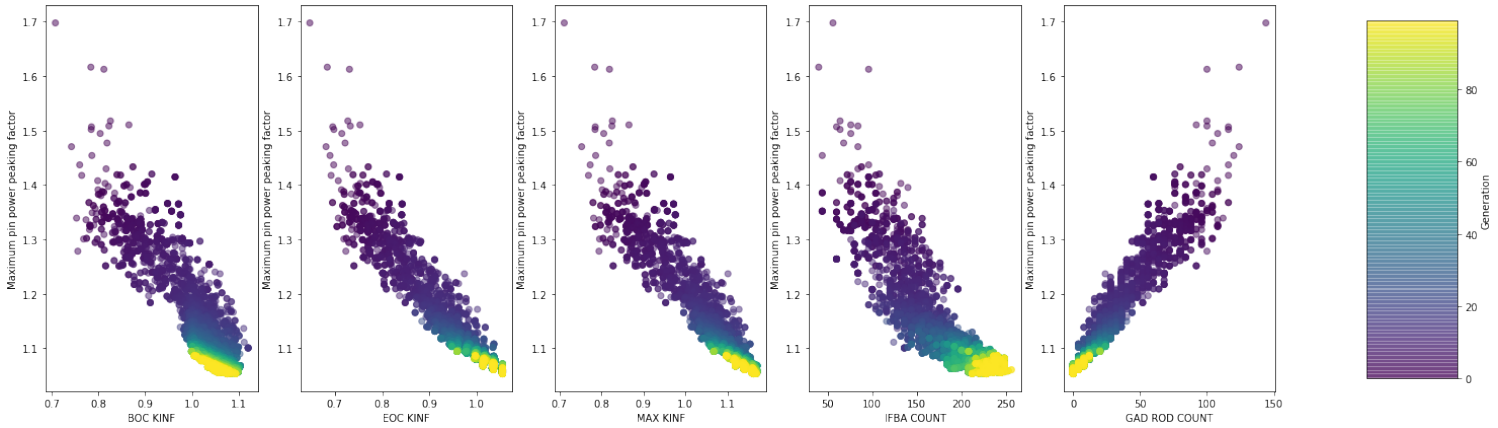

Figure 28. Evolution of NSGA-II–driven optimization of PWR assemblies with 2 wt % Gd_2O_3 pins. The algorithm struggles to increase EOC k_{inf} while keeping BOC in control.

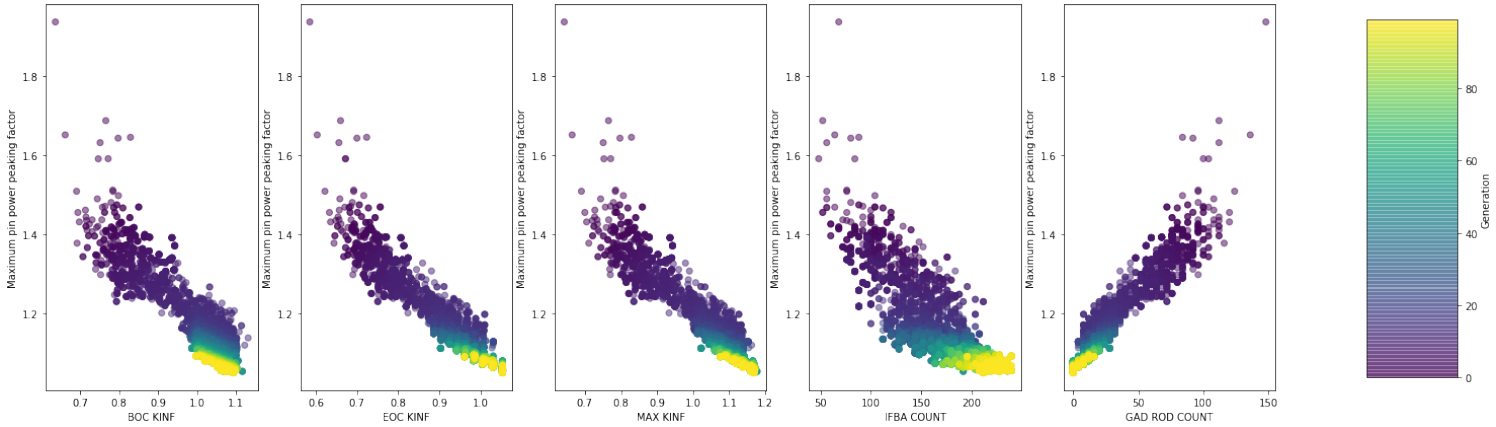

Figure 29. Evolution of NSGA-II–driven optimization of PWR assemblies with 4 wt % Gd_2O_3 pins. The algorithm struggles to increase EOC k_{inf} while keeping BOC in control.

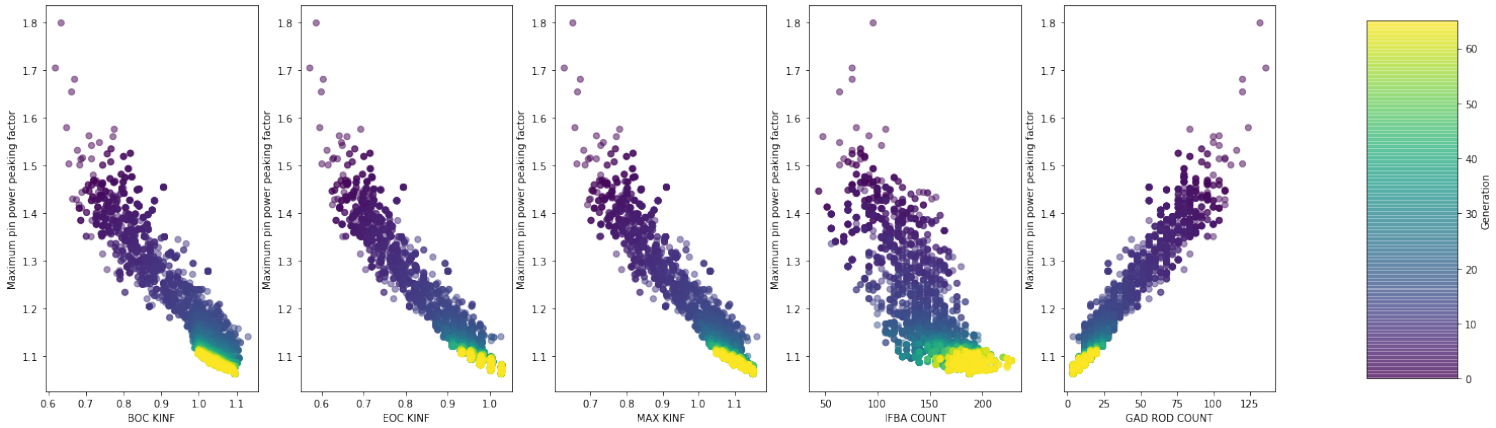

Figure 30. Evolution of NSGA-II–driven optimization of PWR assemblies with 6 wt % Gd_2O_3 pins. The algorithm struggles to increase EOC k_{inf} while keeping BOC in control.

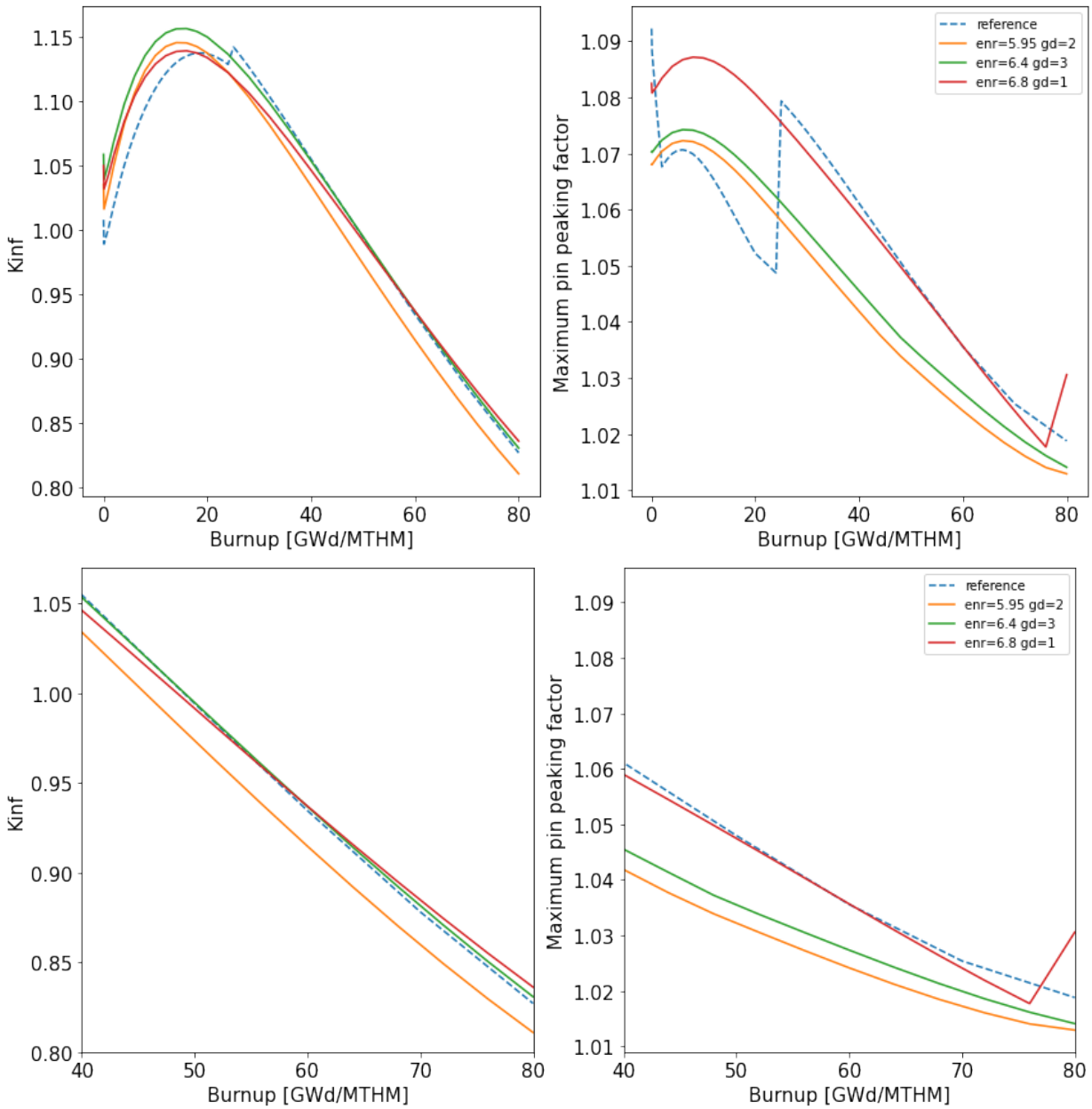

Figure 31. The k_{inf} and maximum PPF curve of three selected designs—two with increased pin enrichment—overlayed with the reference (WABA + IFBA) and design with only IFBA implemented. The bottom images are magnified versions of the top images.

6. LESSONS LEARNED

Throughout this optimization study of LEU+ lattice designs, the authors learned that there is a relationship between analyst heuristics, engineering judgement, and algorithmic exploration. A successful optimization study involves a carefully crafted numerical design space and objective function that guides the optimization algorithm to return a good design in a reasonable time.

One important factor when designing an optimization problem is to reduce the search space as much as possible without harming the potential to find solutions. An example from this work is grouping pins in a lattice and restricting edge pins from having Gd_2O_3. These heuristics are applied to reduce the design space that the algorithm explores.

Another simplification was made when the design space was limited to discrete increments (e.g., enrichment increments of 0.4% ^{235}U and Gd_2O_3 concentration increments of 1%). These simplifications also account for the fabrication cost and uncertainties (i.e., it costs more to fabricate a higher number of unique fuel pins). Increasing the number of pin groups or the discrete number of pin enrichment values might find more optimal lattice design but would take significantly longer to evolve into a feasible design. Additionally, having too vast of a design space might make it more difficult for the algorithm to find a good path to an optimal design.

Similarly, one important aspect of an optimization study is understanding the underlying physics and mechanics of the optimization algorithm. This includes an intuition of the upper and lower limits of the design space and the response (i.e., metric) space. With LEU+ lattice designs, the main focus is to suppress initial excess reactivity without penalizing reactivity in the longer term while placing BAs strategically to avoid high PPFs. This requires understanding the long- and short-term effects of different types of BAs.

Understanding the different types of constraints is also very important in an optimization study. While searching the design space and constructing the optimization problem, identifying which metric is a "hard constraint" vs. a "soft constraint" is crucial for designing a trade-off between two metrics. For example, BOC k_{inf} is a mixed constraint in that—up to a certain point—it can still be tolerated if other more important metrics are improved. Thus, the optimization study must be designed to adequately explore the trade-off of these metrics.

This leads to needing a numerical calculation of the importance of each metric. One of the shortcomings of this work is that the multiple metrics—and the selection of "optimal" design—are qualitatively assessed. However, specific weights can be attributed to aggregate the metrics into one metric, such as operating cost. For example, a dollar value can be attributed for each part per million of soluble boron inserted for excess reactivity control, as well as for extra enrichment of fuel or Gd_2O_3 concentration, to numerically aggregate the metrics to one value. Similarly, the extended cycle length can be converted into a savings in operating cost due to less frequent refueling. This aggregation equation can then be used as an objective function to optimize for the lowest operating cost, which is of ultimate interest.

One less obvious aspect of an optimization study is that it provides data for enhanced analyst intuition. Because optimization runs take several days to several weeks, analysts can monitor design evolution in real time, learn about the metrics' sensitivity to the design parameters, and determine whether the designs are evolving in the correct direction. The optimization problem can then be iterated by modifying the objective function or adjusting the design space, if needed. For example, focusing on reducing maximum PPF hinders the algorithm from increasing the enrichment of edge pins. Reducing the weight on the maximum

PPF violation or setting it as a threshold constraint (e.g., anything below 1.4 is not penalized) allows more focus to be placed on increasing cycle length.

Lastly, optimization studies should be considered guidance and not replace actual design iterations through expert judgement. Automated exploration of the design space using an optimization algorithm generates many data and much insight. These insights should be combined with expert engineering judgement to further optimize the algorithm-designed lattice design.

7. CONCLUSION

This report shows three types of lattice optimization studies for LEU+ lattice designs: (1) GE14 10×10 BWR lattice optimization for multiple maximum enrichment values, (2) Westinghouse 17×17 PWR lattice optimization for IFBA locations to minimize PPFs, and (3) Westinghouse 17×17 PWR lattice optimization to replace WABA insertion with Gd_2O_3 pins.

For this study, the optimization algorithm in MOT drove parameter perturbation, the execution of `Polaris`, and results processing. The optimization studies were designed to perturb only pin enrichment or BA content, not perturb lattice dimensions or operating conditions. The focus of the studies was to increase EOC k_{inf} and proxy for cycle length while maintaining or improving upon initial k_{inf} and peak PPF curve behavior.

Results show that the optimization workflow found feasible designs for the set of constraints provided. The BWR lattice optimization study found BWR lattices with maximum enrichments of 6, 7, 8 , 9, and 10, where BOC k_{inf} was below 1.05, maximum k_{inf} was below 1.15, and maximum PPF was below 1.4. The lattice designs used Gd_2O_3 pins up to 8% and showed increasing k_{inf} values at end of life (EOL) with increasing maximum enrichment constraint. The IFBA location optimization study found IFBA placement that lowered PPFs compared with the reference design and distributed pin power more evenly throughout the lattice. The WABA replacement study found that the longer-term reactivity penalty of Gd_2O_3 pins make it more difficult for Gd_2O_3 to replace WABAs and that additional enrichment is required to meet EOC k_{inf}.

The focus of this work was to develop and demonstrate the capability to reach a feasible, optimal design in a reasonable time frame given a design space and set of constraints and goals. This capability ultimately enables the automated exploration of new design spaces, as performed in the BWR lattice optimization study with increasing enrichment. This capability allows analysts to explore a new design space to understand the sensitivities between parameters and metrics, helping them in the design process.

The optimization package used for this work is available in the ORNL GitLab repository and can be obtained by requesting access from the authors (see Appendix A). This work will be continued for core-level analyses, and the lattices designed in this work will be used for various LEU+ studies, such as used nuclear fuel storage and transportation studies.

8. REFERENCES

[1] C.E. Sanders and J.C Wagner. Study of the Effect of Integral Burnable Absorbers for PWR Burnup Credit (NUREG/CR-6760). Technical Report ORNL/TM-2000-321, U.S. Nuclear Regulatory Commission (NRC), Washington DC, March 2002.

[2] Riley M. (ORCID:0000000196061518) Cumberland, Ryan T. Sweet, Ugur (ORCID:0000000299837809) Mertyurek, Robert Hall, and William A. (ORCID:0000000222117395) Wieselquist. Isotopic and Fuel Lattice Parameter Trends in Extended Enrichment and Higher Burnup LWR Fuel, Volume II: BWR. Technical Report ORNL/TM-2020/1835, Oak Ridge National Lab. (ORNL), Oak Ridge, TN (United States), March 2021.

[3] Bob Hall, Riley Cumberland, William Wieselquist, and Ryan Sweet. Isotopic and Fuel Lattice Parameter Trends in Extended Enrichment and Higher Burnup LWR Fuel Vol I: PWR fuel. Technical Report ORNL/TM-2020/1833, Oak Ridge National Lab. (ORNL), Oak Ridge, TN (United States), February 2021.

[4] Bob Hall, Ryan Sweet, Randy Belles, and William Wieselquist. Extended Enrichment Accident Tolerant LWR Fuel Isotopic and Lattice Parameter Trends. Technical Report ORNL/TM-2021/1961, Oak Ridge National Lab. (ORNL), Oak Ridge, TN (United States), March 2021.

[5] Nuclear Regulatory Commission. LaSalle, Units 1&2, Updated Final Safety Analysis Report, Revsion 20, Chapter 4, Reactor. Technical Report ML14113A088, Nuclear Regulatory Commission, Washington D.C. United States, 2014.

[6] Michael L. Fensin. *OPTIMUM BOILING WATER REACTOR FUEL DESIGN STRATEGIES TO ENHANCE EACTOR SHUTDOWN BY THE STANDBY LIQUID CONTROL SYSTEM*. PhD thesis, University of Florida, Gainesville, FL, United States, 2004.

[7] Alejandro Castillo, Cecilia MartÃŋn-del Campo, JosÃl'-Luis Montes-Tadeo, Juan-Luis FranÃğois, Juan-JosÃl' Ortiz-Servin, and RaÃžl PerusquÃŋa-del Cueto. Comparison of heuristic optimization techniques for the enrichment and gadolinia distribution in BWR fuel lattices and decision analysis. *Annals of Nuclear Energy*, 63:556–564, January 2014.

[8] Cecilia Martin-del Campo, Juan Luis FranÃğois, Roberto Carmona, and Ivonne P. Oropeza. Optimization of BWR fuel lattice enrichment and gadolinia distribution using genetic algorithms and knowledge. *Annals of Nuclear Energy*, 34(4):248–253, April 2007.

[9] Juan JosÃl' Ortiz-Servin, David A. Pelta, JosÃl' Manuel Cadenas, and Alejandro Castillo. A new methodology to speed-up fuel lattice design optimization using decision trees and new objective functions. *Annals of Nuclear Energy*, 161:108445, October 2021.

[10] Majdi I. Radaideh, Isaac Wolverton, Joshua Joseph, James J. Tusar, Uuganbayar Otgonbaatar, Nicholas Roy, Benoit Forget, and Koroush Shirvan. Physics-informed reinforcement learning optimization of nuclear assembly design. *Nuclear Engineering and Design*, 372:110966, February 2021.

[11] US NRC. LaSalle, Units 1 & 2, Submittal of Updated Final Safety Analysis Report (UFSAR), Revision 20, Chapter 4. Technical Report ML14113A088, US NRC, April 2014.

[12] D. J. Kelly. Depletion of a BWR lattice using the racer continuous energy Monte Carlo code. December 1995. Number: CONF-950420- Publisher: American Nuclear Society, Inc., La Grange Park, IL (United States).

[13] W. A. Wieselquist, R. A. Lefebvre, and M. A. Jessee. SCALE Code System. Technical Report ORNL/TM-2005/39, Oak Ridge National Laboratory, Oak Ridge, TN, 2020.

[14] I. Variansyah, J. W. Bae, B. R. Betzler, and G. Ilas. Metaheuristic Optimization Tool. Technical Report ORNL/TM-2019/1443, Oak Ridge National Laboratory, Oak Ridge, Tennessee, USA, March 2020.

[15] K. Deb, A. Pratap, S. Agarwal, and T. Meyarivan. A fast and elitist multiobjective genetic algorithm: NSGA-II. *IEEE Transactions on Evolutionary Computation*, 6(2):182–197, 2002.

[16] The pandas development team. pandas-dev/pandas: Pandas, February 2020.

[17] IAEA. Characteristics and Use of Urania-gadolinia Fuels. Technical Report IAEA-TECDOC-844, International Atomic Energy Agency, Vienna, Austria, November 1995.

[18] J. Hu, U. Mertyurek, A. Bielen, and W. A. Wieselquist. Assessment of Core Physics Characteristics of Extended Enrichment and Higher Burnup LWR Fuels Using the Polaris/PARCS Two-Step Approach Vol. 1: PWR Fuel. Technical Report ORNL/TM-2022/1831, Oak Ridge National Lab. (ORNL), Oak Ridge, TN (United States), 2022.

APPENDIX A. GITLAB REPOSITORY LINK AND DESCRIPTION

The optimized designs generated in this work are uploaded in the ORNL GitLab repository. The link is `https://code.ornl.gov/scale/analysis/mlgen-lattice/`, and access can be requested by contacting the the authors of this report.

The repository contains `Polaris` input and output files for the following designs:

- GE14 10×10 BWR lattice design
  - Lattice design with maximum pin enrichment 5,6,7,8,9, and 10
- Westinghouse 17×17 PWR lattice design
  - Lattice design with maximum pin enrichment 5.95% with 200 IFBA pins
  - Lattice design with maximum pin enrichment 5.95% with 80 IFBA pins

Each directory contains the corresponding design's `Polaris` files. Below is the list of file extensions and the file description.

- `.f71`: `SCALE` material composition file
- `.inp`: `SCALE/Polaris` input file
- `.msg, .out`: Message and output file from the `Polaris` run
- `.t16`: `SCALE` nodal data file containing reactivity and local pin peaking factors
- `.png`: `Polaris`-generated lattice image
- `.f33`: `SCALE` cross section library
- `.idc`: `Polaris` input parameters